



Contents lists available at ScienceDirect

Journal of Orthopaedic Translation

journal homepage: www.journals.elsevier.com/journal-of-orthopaedic-translation

Controlled growth factor delivery system with osteogenic-angiogenic coupling effect for bone regeneration



Fei Kang^{a,b,1}, Qiying Yi^{b,1}, Pengcheng Gu^b, Yuhan Dong^b, Ziyang Zhang^b, Lijuan Zhang^b, Yan Bai^{b,*}

^a Department of Biomedical Materials Science, Third Military Medical University, Chongqing, 400038, China

^b School of Pharmacy, Chongqing Medical University, Chongqing, 400016, China

ARTICLE INFO

Keywords:

Growth factor
Dual release
Cell communication
Bone regeneration

ABSTRACT

Objective: Bone regeneration involves a coordinated cascade of events that are regulated by several cytokines and growth factors, among which bone morphogenic protein-2 (BMP-2), vascular endothelial growth factor (VEGF) and fibroblast growth factor-2 (FGF-2) play important roles. In this study, we investigated the effects of dual release of the three growth factors on bone regeneration in femur defects.

Methods: A composite consisting of Gelatin microparticles loaded with VEGF/FGF-2 and poly(lactic-co-glycolic acid)-poly(ethylene glycol)-carboxyl (PLGA-PEG-COOH) microparticles loaded with BMP-2 encapsulated in a nano hydroxyapatite-poly lactic-co-glycolic acid (nHA-PLGA) scaffold was prepared for the dual release of the growth factors.

Results: On the 14th day, decreased release rate of BMP-2 compared with FGF-2 and VEGF was observed. However, after 14 days, compared to FGF-2 and VEGF, BMP-2 showed an increased release rate. Controlled dual release of BMP-2 and VEGF, FGF-2 resulted in a significant osteogenic differentiation of bone mesenchymal stem cells (BMSCs). Moreover, effects of the composite scaffold on functional connection of osteoblast-vascular cells during bone development were evaluated. The synergistic effects of dual delivery of growth factors were shown to promote the expression of VEGF in BMSCs. Increased secretion of VEGF from BMSCs promoted the proliferation and angiogenic differentiation of human umbilical vein endothelial cells (HUVECs) in the co-culture system. At 12 weeks after implantation, blood vessel and bone formation were analyzed by micro-CT and histology. The composite scaffold significantly promoted the formation of blood vessels and new bone in femur defects.

Conclusions: These findings demonstrate that dual delivery of angiogenic factors and osteogenic factors from Gelatin and PLGA-PEG-COOH microparticles-based composite scaffolds exerted an osteogenic-angiogenic coupling effect on bone regeneration. This approach will inform on the development of appropriate designs of high-performance bioscaffolds for bone tissue engineering.

1. Introduction

In clinical medicine, regeneration of large bone defects caused by tumor resection, skeletal trauma, or infections is a significant challenge [1]. The bone development and repair process is precisely regulated by a large number of cells and growth factors [2]. Among all the growth factors, bone morphogenetic proteins-2 (BMP-2), vascular endothelial growth factor (VEGF) and fibroblast growth factor-2 (FGF-2) play very important roles in bone formation. Due to its high osteoinductive potential, BMP-2 plays a central role in most bone regeneration strategies

[3]. It initiates the complete process of bone construction, such as the proliferation and differentiation of osteoblasts, osteoclasts and mesenchymal cells [4]. VEGF, one of the most important angiogenic factors, is involved in angiogenesis and bone formation [5,6]. FGF-2 is the most effective pro-cytogenetic factor. It promotes angiogenesis, wound healing and tissue damage repair [7]. Moreover, it induces endothelial cells to germinate and proliferate, and increases vascular permeability [8,9].

Since the induction effects and mechanisms of various growth factors are different, BMP-2, VEGF and FGF-2 are respectively involved in distinct phases of bone formation [10]. During normal bone healing,

* Corresponding author. School of Pharmacy, Chongqing Medical University, District of Yuzhong, Chongqing, 400016, PR China.

E-mail address: baian1226@163.com (Y. Bai).

¹ Contributed equally to this paper.

<https://doi.org/10.1016/j.jot.2021.11.004>

Received 31 August 2021; Received in revised form 1 November 2021; Accepted 15 November 2021

VEGF expression peaks during the early days while BMP expression peaks at later time points [11–15]. Our investigations proved that there is a preferred sequence of VEGF, FGF-2 and BMP-2 during the osteogenic differentiation of bone mesenchymal stem cells (BMSCs). The addition of both FGF-2 and VEGF in the early differentiation stage, and BMP-2 in the late differentiation stage was shown to significantly enhance osteoblastic differentiation of BMSCs [16]. Therefore, to mimic the signaling cascades and expressions of different growth factors during bone repair, a composite scaffold that could realize sequential release of growth factors should be constructed based on the predetermined profile. A novel advanced scaffold that is capable of fast releasing VEGF and FGF-2, followed by a slow and sustained release of BMP-2 might be a potential way for cellular osteoinduction and bone regeneration. Controlled release of growth factors from bioscaffolds maybe advantageous for sequential application of proteins and molecules during tissue damage repair, which will be an important strategy for investigating the regulation of regenerative processes in clinical medicine.

Apart from osteoinduction, functional microvascular networks are crucial for bone regeneration. They provide oxygen and nutrients to facilitate growth, differentiation, and tissue functionality. During bone development and growth, osteogenesis and vascularization are coupled and mutually promote each other [17]. Intimate functional interactions between endothelial cells/endothelial progenitor cells and bone-forming cells demonstrate the close association between angiogenesis and osteogenesis [18,19]. Autocrine or paracrine growth factors have been used to mediate interactions between endotheliocytes and osteoblasts in bone regenerative processes [20,21]. Studies have proven the synergistic regulation of BMPs, FGF-2 and VEGF on cell communication during osteogenesis and angiogenesis. Cross-communication between BMSCs and endothelial cells (ECs) influence osteogenic differentiation and enhance the bone healing [22]. ECs stimulate the migration and differentiation of Osteoblasts (OBs) by producing BMP-2 [23]. Moreover, FGF-2 induced VEGF secretion by OBs stimulated the proliferation of ECs and the secretion of matrix metal proteinases [24]. These studies proved that angiogenesis and osteogenesis were regulated coupling due to the actions of growth factors on bone and endothelial cells. Therefore, we hypothesized that functional interactions between endothelial and bone marrow stromal cells of relevance to bone tissue engineering can be promoted by localized regulation of growth factors from scaffolds. We tested this hypothesis by co-culturing BMSCs and human umbilical vein endothelial cells (HUVECs) in a composite scaffold with temporal delivery of FGF-2, VEGF and BMP-2.

In this study, Gelatin microparticles (Gelatin_{mp}) and PLGA-PEG-COOH microparticles (PLGA-PEG-COOH_{mp}) were developed and characterized. Different degrading rates of Gelatin and PLGA-PEG-COOH were used to achieve the temporary release of therapeutic biomolecules. In this study, VEGF and FGF-2 were encapsulated in Gelatin_{mp}, while BMP-2 was encapsulated in PLGA-PEG-COOH_{mp}. Then, composite nHA-PLGA porous scaffolds containing VEGF/FGF-2-loaded Gelatin_{mp} and BMP-2-loaded PLGA-PEG-COOH_{mp} were fabricated using a supercritical CO₂ (scCO₂) foaming technology. We hypothesized that dual delivery of VEGF and FGF-2 followed by BMP-2 from a composite scaffold enhances new bone formation. Therefore, we investigated the osteoinductive effects of dually delivered growth factors on BMSCs *in vitro*, and their effects on communication as well as functional interactions of osteoblast-vascular cells during bone development. Finally, we established the femur defect rat models to evaluate osteogenic and angiogenic effects of the composite scaffold *in vivo*. New bone formation after implantation of the scaffold were investigated and quantitatively analyzed by micro-CT (μ -CT) and histological staining. The polymeric scaffolds developed in this study realized the temporal delivery of different growth factors, and are therefore, a potential strategy for investigating the tissue regeneration and development process.

2. Materials and methods

2.1. Materials

PLGA-PEG-COOH (PLGA, $M_w = 10$ kDa, PEG, $MW = 2000$, 50:50) was purchased from Nano soft polymers. PLGA ($M_w = 100$ kDa, 50:50) were purchased by Dai gang Biomaterial Co. Ltd (Jinan, Shandong Province, China). Gelatin type-B ($MW = 40,000$), PEG ($MW = 1000$), sodium metabisulfite, MES buffer, N-ethyl-N'-(3-dimethylaminopropyl) carbodiimide hydrochloride (EDC), N-hydroxysulfosuccinimide sodium salt (NHS), Alizarin red S (ARS), and tris hydrochloride (Tris-HCl) buffer were purchased from Sigma-Aldrich (St Louis, MO, USA). VEGF, BMP-2 and FGF-2 were purchased from PeptoTech Inc (Rocky Hill, NJ, USA) and quantitative ELISA kits were purchased from R&D Systems (Minneapolis, MN, USA). Matrigel was purchased from BD Biosciences (Franklin Lakes, NJ, USA). Dulbecco's modified Eagle's medium (DMEM), trypsin and fetal bovine serum (FBS) were purchased from HyClone (Logan, UT, USA).

2.2. Cell culture

BMSCs were isolated from the bone marrow of 6-week-old rats. First, adherent soft tissues and epiphyses were cleared. Then, a syringe needle was inserted into one end of the bone and washed into the culture dish with complete culture medium to obtain the bone marrow. Cells were centrifuged, counted and seeded in a culture plate with DMEM media supplemented with 10% FBS. Incubation was done at 37 °C in 95% humidified air and 5% CO₂. Cells were cultured for three passages and used in experiments. HUVECs were maintained in DMEM containing 10% FBS, and 1% antibiotics (80 U/mL penicillin and 80 μ g/mL streptomycin). The 2 to 5 generations of HUVECs were used for further analyses.

2.3. Fabrication of BMP-2-PLGA-PEG-COOH_{mp}/VEGF-FGF-2-gelatin_{mp}/nHA-PLGA scaffolds

Addition of FGF-2 and VEGF during the early proliferation stage and BMP-2 during the differentiation stage of BMSCs has been shown to effectively promote osteogenesis [25]. In bone repair models, osteogenesis occurs after angiogenesis, while VEGF expression is significantly increased at 5–14 days [26,27]. Therefore, to simulate the expressions of growth factors during bone formation, we developed a new scaffold that could quickly release FGF-2 and VEGF, while slowly releasing BMP-2. The scaffold consisted of two compartments. One compartment rapidly released VEGF and FGF-2 while the other compartment slowly released BMP-2. To realize the distinct release kinetics, Gelatin_{mp} and PLGA-PEG-COOH_{mp} were used as biodegradable carriers for VEGF/FGF-2 and BMP-2, respectively. The nHA-PLGA component formed the continuous phase of the scaffold, which was embedded with Gelatin_{mp} and PLGA-PEG-COOH_{mp}.

The fabrication processes of growth factor loaded Gelatin_{mp} and PLGA-PEG-COOH_{mp} are shown in Fig. 1a. For Gelatin_{mp} fabrication, 100 mg Gelatin powder was dissolved in 10 mL deionized water after which the pH of the mixture was adjusted to 7.00 using 0.2 M sodium hydroxide solution. Under controlled stirring, water was gradually replaced by ethanol and cross-linked with glyoxal for 10 h to form Gelatin_{mp}. The unreacted aldehyde group of glyoxal was quenched using sodium pyrosulfite aqueous solution. Gelatin_{mp} was obtained by centrifugation at 12 000 g for 90 min and lyophilized using a freeze dryer. For PLGA-PEG-COOH_{mp} fabrication, 50 mg PLGA-PEG-COOH was added into 8 mL DMSO, then, the mixture was dialyzed using a dialysis tube against deionized water for self-assembly. Dialyzed water was changed every 2–4 h. After 24 h, PLGA-PEG-COOH_{mp} was obtained by centrifugation and lyophilized. The MES buffer, supplemented with EDC and NHS salt, was used to activate COOH- of microparticles at room temperature for 1

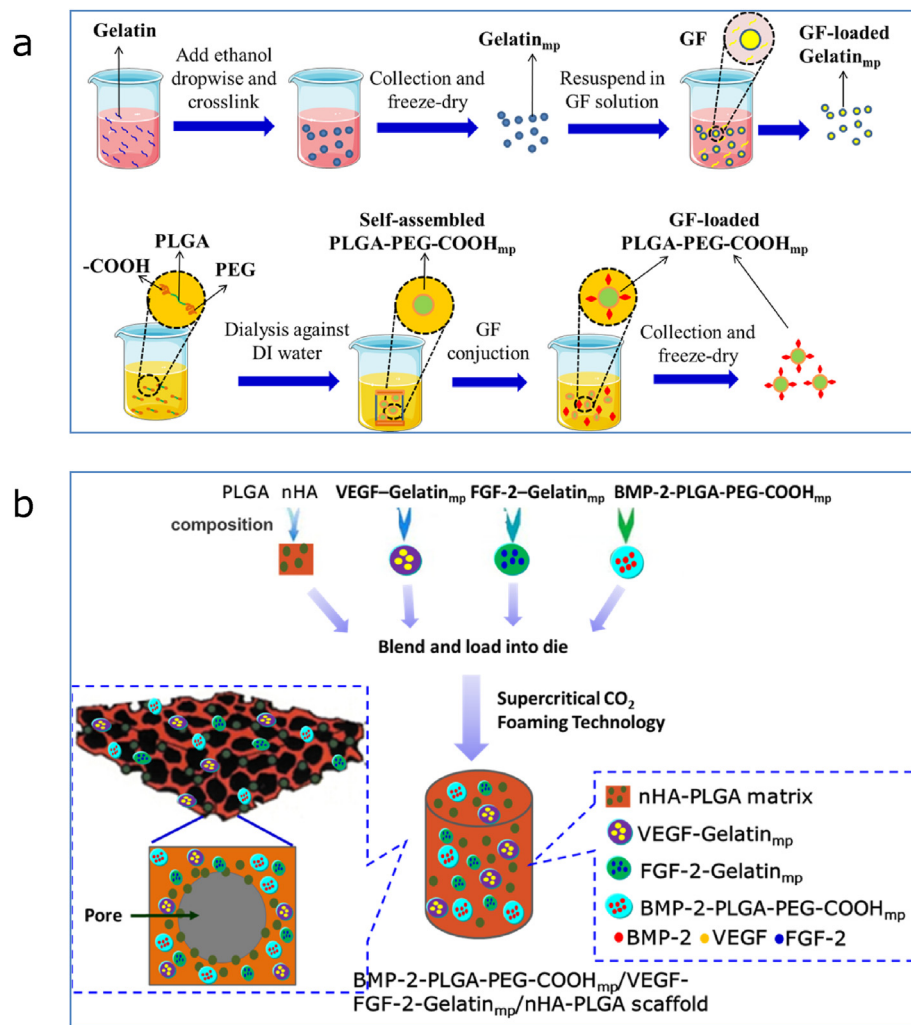


Figure 1. Fabrication Schematics of growth factor-loaded microparticles and scaffolds. (a) Fabrication of gelatin and PLGA-PEG-COOH microparticle (mp) and growth factor (GF) loading. (b) Fabrication of BMP-2-PLGA-PEG-COOH_{mp}/VEGF-FGF-2-Gelatin_{mp}/nHA-PLGA scaffolds.

h. Based on effective concentrations of FGF-2, VEGF and BMP-2 [25–31], 10 mg of activated Gelatin_{mp} and PLGA-PEG-COOH_{mp} was added to the FGF-2, VEGF and BMP-2 solution (20 µg/mL of each growth factor) and reacted at 4 °C overnight to graft with growth factors. The growth factor loaded microparticles were centrifuged and lyophilized.

The BMP-2-PLGA-PEG-COOH_{mp}/VEGF-FGF-2-Gelatin_{mp}/nHA-PLGA scaffold was fabricated using a supercritical CO₂ foaming technology as shown in Fig. 1b [28]. Briefly, BMP-2-PLGA-PEG-COOH_{mp}, VEGF-Gelatin_{mp} and FGF-2-Gelatin_{mp} (mass ratio of 5:1:1) were physically mixed with nHA and a PLGA polymer powder and foamed by scCO₂ at 8 Mpa, 33 °C to form the BMP-2-PLGA-PEG-COOH_{mp}/VEGF-FGF-2-Gelatin_{mp}/PLGA scaffold. With pressure release, pores were created in the polymer structure, thereby fabricating a porous composite scaffold with encapsulated BMP-2-PLGA-PEG-COOH_{mp}, VEGF-Gelatin_{mp} and FGF-2-Gelatin_{mp}.

2.4. Characterization of the microparticles and scaffolds

Morphologies of the microparticles and scaffolds were observed by scanning electron microscopy (SEM) (JEOLT330A, JEOL, Ltd., Peabody, MA). Briefly, micro particles and scaffolds were stuck on the sample stage, after which the ion sputtering coating method was used for gold-palladium coating. Then, coated samples were tested and imaged. The porous nHA-PLGA scaffold seeded with BMSCs was observed by Laser scanning confocal microscopy (LSCM) at 25 °C, using Zetasizer (Malvern,

Nano ZS, USA) to examine particle sizes of the microspheres at a light scattering angle of 90°. Encapsulation efficiencies and loading capacities of BMP-2-PLGA-PEG-COOH_{mp} were measured by extraction using CH₂CL₂. BMP-2-PLGA-PEG-COOH_{mp} was dissolved in 1000 µL CH₂CL₂. Then, the mixture was added into 2 mL PBS (pH 7.4) and vigorously shaken for 2–3 min to extract BMP-2 into PBS. The aqueous solution was obtained by centrifugation at 4000g, after which BMP-2 concentrations were determined using an ELISA kit. To quantitatively analyze FGF-2 and VEGF loaded in Gelatin_{mp}, Gelatin_{mp} was dissolved in PBS containing 1 mg/mL collagenase and centrifuged at 12,000 g for 15 min. Then, the supernatant was collected and concentrations of FGF-2 and VEGF in MPs were detected using ELISA kits.

2.5. Release kinetics of FGF-2, VEGF and BMP-2

In this assay, 10 mg BMP-2-PLGA-PEG-COOH_{mp}, VEGF-Gelatin_{mp} and FGF-2-Gelatin_{mp} were dissolved in 1.0 mL PBS solution and incubated at 37 °C under shaking at 100 rpm. Then, 0.5 mL of the mixed solution was used to assess the release rates of the three growth factors in the microparticles. The BMP-2-PLGA-PEG-COOH_{mp}/VEGF-FGF-2-Gelatin_{mp}/nHA-PLGA scaffold was cut into quarters, incubated with 1 antimicrobial/antibiotic solution, washed 3 times and placed in a centrifuge tube containing 1 mL PBS (pH 7.4). The sample was incubated at 37 °C and under shaking at 100 rpm. The supernatant was obtained at pre-determined intervals and stored at –80 °C. Then, the scaffold was

resuspended in 1 mL fresh PBS and incubated to the next time point. Release rates of the growth factors were measured using ELISA kits.

2.6. *In vitro* studies: effects of BMP-2-PLGA-PEG-COOH_{mp}/VEGF-FGF-2-gelatin_{mp}/nHA-PLGA scaffold on differentiation of BMSCs

2.6.1. Cell proliferation

Cell proliferation was assessed using the CCK-8 solution. Briefly, CCK-8 (10 µL) was added into each well. Cells were incubated for 1 h at 37 °C. The SpectraMax Plus reader (Molecular Devices, Sunnyvale) was used to determine the absorbance of the medium at 450 nm.

2.6.2. Cell-cycle analysis

After 14 days of cultivation, BMSCs were harvested and fixed in 70% ethanol at –20 °C overnight. Fixed cells were washed using PBS and stained with 10 µg/mL RNase and 5 µg/mL propidium iodide at 37 °C for 30 min. After staining, DNA concentrations in cells at different stages of division were measured by flow cytometry.

2.6.3. Cell ultrastructure assay

Ultrastructures of BMSCs were observed by transmission electron microscopy. BMSCs ($2 \times 10^4/\text{cm}^2$) were seeded on a BMP-2-PLGA-PEG-COOH_{mp}/VEGF-FGF-2-Gelatin_{mp}/nHA-PLGA scaffold or a nHA-PLGA scaffold (without growth factors) and incubated for 21 days. BMSCs were washed twice using PBS, harvested and fixed in 0.5% precooled glutaraldehyde for 30 min at 4 °C. The sample was centrifuged at 13,000 rpm for 15 min at 4 °C. The supernatant was discarded and cells were fixed in 3% glutaraldehyde at 4 °C. Then, cell samples were fixed in 1% osmium tetroxide, dehydrated in acetone, embedded and sliced. Cells were dyed with uranium acetate and lead citrate. Ultrastructural changes in cells were observed and imaged by a transmission electron microscopy attached to a digital camera ($\times 8000$).

2.6.4. ALP activity staining and assay

To stain for ALP activities, BMSCs were incubated to various points, washed twice, and fixed in 4% paraformaldehyde using 0.1% Trinton-X100 in PBS, after which they were stained with 5-bromo-4-chloro-3-indolyl phosphate and nitro blue tetrazolium for 30 min. To quantify ALP activities, samples were washed using PBS and lysed through three cycles of freezing and thawing. Cell lysates were centrifuged for 1 min at 13,000 rpm. Then, 20 µL supernatants were used to evaluate ALP activities, and ALP contents were analyzed using ALP activity kit.

2.6.5. Alizarin red S (ARS) staining and mineralization assay

BMSCs were harvested, washed, fixed in 4% paraformaldehyde, rinsed and stained with ARS for 10 min. Alizarin red S stained cells were extracted using 500 µL mixed solution of acetic acid (1.4 mM) and ethanol (3.4 mM). Concentrations of extracted ARS were tested by measuring absorbance at 450 nm to determine the mineralization degree.

2.6.6. RNA extraction and quantitative real-time PCR

The mRNA expression levels of osteogenic genes and angiogenic factors in BMSCs were measured by qRT-PCR. The trizol reagent (Takara) was used to extract total RNA from BMSCs according to the manufacturer's protocols. Reverse transcription was performed using the reverse transcription kit (Takara) according to the manufacturer's instructions. The primers used in this study were shown in Table S1. SYBR Premix Ex Taq II (TaKaRa) was used as the fluorescent probe to perform RT-PCR on a BIO-RAD RT-System. Real-time PCR conditions were: 94 °C for 30 s, followed by 40 cycles at 94 °C for 5 s, 60 °C for 30 s 40 cycles of 94 °C for 5 s, and 60.5 °C for 34 s. There were 40 cycles of denaturation at 95 °C for 5 s and amplification at 60 °C for 24 s. Assays were performed in triplicates. Expression levels of all mRNAs were calculated by the normalization to that of GAPDH.

Table 1

Characterization of growth factors loaded microparticles.

Microparticles	Encapsulation efficiency(%)	Loading capacity(%)	Mean size(µm)
FGF-2-Gelatin _{mp}	66.33	2.01×10^{-3}	44.85
VEGF-Gelatin _{mp}	65.87	1.96×10^{-3}	47.79
BMP-2-PLGA-PEG-COOH _{mp}	75.69	1.13×10^{-3}	54.85

2.6.7. Quantitative analysis of proteins

BMSCs were seeded on scaffolds in 24 well plates. Then, these high expressed angiogenic factors in BMSCs were analyzed using ELISA kits according to the manufacturer's instructions.

2.7. Effects of the BMP-2-PLGA-PEG-COOH_{mp}/VEGF-FGF-2-gelatin_{mp}/nHA-PLGA scaffold on functional associations of osteoblast-vascular cells in the co-culture system

Effects of dual FGF-2, VEGF and BMP-2 released from the composite scaffold on functional associations of osteoblast-vascular cells in a co-cultured system were evaluated using the transwell non-contact co-culture system. BMSCs were seeded on scaffolds and cultured in the apical compartment, while HUEVCs were cultured in the basolateral compartment.

2.7.1. Assessments of cell proliferation and expressions of angiogenic differentiation genes

The BMSCs seeded scaffold was co-cultured with HUVECs in 24-well plates for 14 days, after which cell proliferation was determined by the CCK-8 assay. Expression levels of vasculogenic genes (vWF, VEGFR and PECAM-1) in HUVECs were evaluated by real-time quantitative PCR. The primers used in this experiment were shown in Table 1. RNA extraction and quantitative real-time PCR were performed as described in section 2.6.6.

2.7.2. Quantitative analysis of MMP-2 and MMP-9 protein levels

HUVECs were cultured in the present of scaffolds seeded with BMSCs in 24-well plates for 14 days. Protein concentrations of MMP-9 and MMP-2 were evaluated using ELISA kits as the manufacturer's instructions.

2.7.3. Wound - healing assay

The scaffold implanted with BMSCs was co-cultured with HUVECs in 24-well plates for 14 days. Then, a sterilized pipett tip was used to scrape the HUVEC monolayer on the culture plate. After gentle washing using PBS, cells were cultured in serum-free medium. HUVECs migration distances were measured after culturing for 16 h at 37 °C by obtaining images.

2.7.4. Tube formation assay

HUVECs were co-cultured with scaffolds seeded with BMSCs for 14 days. Briefly, a matrigel without growth factors was melted on ice overnight, and evenly spread on each well and polymerized at 37 °C for 1 h. HUVECs were seeded on the matrigel and after 24 h of co-cultivation, tube formation was observed and imaged by an inverted microscope. The image Pro Plus software was used to measure the total length of tubular structure.

2.7.5. Cell invasion assay

The cell invasion assay was performed in 24-well cell incubators using inserts with 8 µm sized pore chambers. The upper surface of the insert was coated with Matrigel. Scaffolds seeded with BMSCs were incubated in the bottom chamber. HUVECs were seeded in the upper chamber and cultured for 24 h. Non-passing cells were cleared by moistened cotton swabs from the upper chamber. Cells that had invaded the lower surface

were fixed in cold methanol and stained by crystal violet. The filter was rinsed using distilled water, after which crystal violet was removed by acetic acid and their absorbance was determined at 590 nm.

2.7.6. VEGFR inhibition

The HUVECs were incubated with BMSCs in a non-contact manner. A suspension of BMSCs was added to BMP-2-PLGA-PEG-COOH_{mp}/VEGF-FGF-2-Gelatin_{mp}/nHA-PLGA scaffolds and non-loaded scaffolds, after which they were cultured in the apical compartment. HUVECs in the basolateral compartment were treated DMEM medium supplied with 10 μ M JK-P3. The HUVECs were harvested for qRT-PCR and CCK-8 assay.

2.8. In vivo assay

2.8.1. Establishment of animal models and scaffold implantation

Animal experiments were approved by the Laboratory Animal Welfare and Ethics Committee of Chongqing Medical University, China (SCXK2018-0003). Twelve-week old female Sprague Dawley rats weight 300–320 g were used in these experiments. Briefly, normal rats were anesthetized with pentobarbital sodium (75 mg/kg). Four weeks after ovariectomy, osteoporotic rats were randomized into four groups: blank (unfilled defect), nHA-PLGA scaffold, BMP-2/VEGF/FGF-2/nHA-PLGA scaffold (BVF/nHA-PLGA scaffold), BMP-2-PLGA-PEG-COOH_{mp}/VEGF-FGF-2-Gelatin_{mp}/nHA-PLGA scaffold (B-PPC_{mp}/VF-GEL_{mp}/nHA-PLGA scaffold). After exposure of the lateral femoral condyle, implant holes with a diameter of 2.5 mm and a depth of 3 mm were drilled on two femoral condyles using a dental drill. Then, cylindrical scaffolds were implanted into cavity defects. The blank group was subjected to surgery, but without scaffold implantation. Finally, wounds were carefully sutured to ensure animal safety. At postoperative week 12, the two femur condyles were obtained and stored in 4% paraformaldehyde for further analyses.

2.8.2. Micro-CT

Immediately after the acquisition process, the same system was used to obtain μ -CT images of samples at 80 kV and 100 μ A. The μ -CT images were further analyzed by using the VGStudio Max 2.2 software. To

distinguish between bones and implants, a CT cut-off value was determined to distinguish between the pocket and host bone in the specimen, after which three-dimensional (3D) reconstruction was performed. Micro-CT parameters of bone repair within femur defects, including tissue volume (TV, mm³), bone volume (BV, mm³), bone volume fraction (BV/TV, %), structural model index (SMI), trabecular bone thickness (Tb.Th, μ m), trabecular bone number (Tb.N, 1/mm), trabecular bone spacing (Tb.Sp, μ m) and bone mineral density (BMD, g/cm³) were evaluated to determine osteogenic abilities of the scaffolds.

2.8.3. Histological and immunohistochemical examination

After micro-CT scanning, bone specimens were fixed in 4% paraformaldehyde at 4 °C for 3 days, decalcified using 10% ethylenediaminetetraacetic acid (EDTA) in PBS for 14 days, and embedded in paraffin. Then, each paraffin block was sliced into 5 μ m thick sections and stained with hematoxylin and Masson. For immunohistochemical staining of CD31, sections were incubated with anti-CD31 antibodies at 4 °C overnight, after which they were stained for 2 h at room temperature with secondary antibodies. The color was developed using a horseradish peroxidase substrate detection kit and counterstained with hematoxylin. Finally, tissue sections were observed by microscopy.

2.9. Statistical analysis

Data are expressed as means \pm standard deviation for $n = 3$. Statistical analyses were performed using the IBM SPSS software. Thresholds for significance were: * $p < 0.05$, ** $p < 0.01$, *** $p < 0.001$ and **** $p < 0.0001$.

3. Results

3.1. Characteristics of the microparticles and scaffolds

Fig. 2a–c showed SEM images of PLGA-PEG-COOH_{mp}, Gelatin_{mp} and nHA-PLGA scaffolds, respectively. PLGA-PEG-COOH_{mp} exhibited irregular spherical shapes and smooth surfaces. While Gelatin_{mp} exhibited irregular flake particles with a smooth surface. Mean sizes of PLGA-PEG-

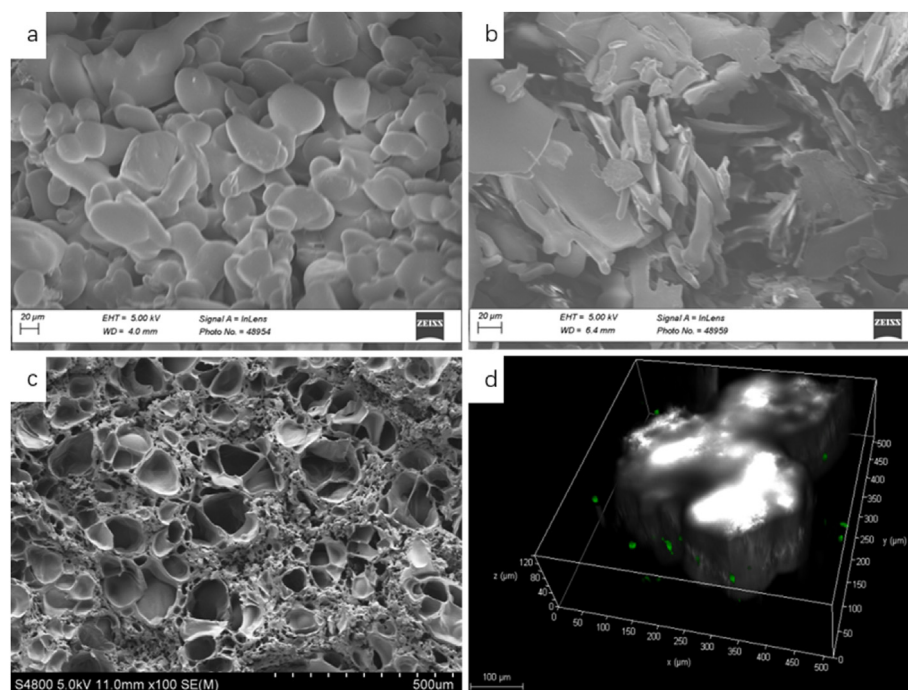


Figure 2. Morphology of microparticle and scaffold. (a) SEM image of PLGA-PEG-COOH_{mp}. (b) SEM image of Gelatin_{mp}. (c) SEM image of Porous nHA-PLGA scaffolds. (d) LSCM 3D image of Porous nHA-PLGA scaffolds seeded with BMSCs. The white areas were the pores in scaffold, green spots were BMSCs in scaffolds.

Table 2
Characterization of microparticles encapsulated scaffolds.

Scaffold	Mean pore size (μm)	Pore size rang (μm)	Porosity (%)	Compressive strength(MPa)
BMP-2-PLGA-PEG-COOH _{mp} /VEGF-FGF-2-Gelatin _{mp} /nHA-PLGA scaffold	143.33	100–200	74.96	10.53

COOH_{mp} and Gelatin_{mp} were 54.85 and 44.85 μm , respectively (Table 1). Mechanical properties of the composite scaffold materials were satisfactory. Their mean porosity, pore sizes and compressive strengths were $74.96 \pm 1.62\%$, 100–200 μm and 10.53 ± 2.67 MPa, respectively (Table 2). Encapsulation efficiency of VEGF- Gelatin_{mp}, FGF-2-Gelatin_{mp} and BMP-2-PLGA-PEG-COOH_{mp} was 65.87, 66.33 and 75.69%, respectively. Fig. 2d showed the LSCM 3D image of porous nHA-PLGA scaffolds seeded with BMSCs. White areas denoted pores in the scaffold, while green spots denoted BMSCs in the scaffold. The 3D image further showed the porous structure of the nHA-PLGA scaffold, with BMSCs growing in the pores.

3.2. *In vitro* release kinetics of FGF-2, VEGF and BMP-2 from microparticles and composite scaffolds

Fig. 3a showed the release behaviors of FGF-2, VEGF and BMP-2 from the PLGA-PEG-COOH_{mp} and Gelatin_{mp} for three weeks. The release rate of VEGF and FGF-2 from Gelatin_{mp} was faster (70.18 and 71.33%) than that of BMP-2 from PLGA-PEG-COOH_{mp} (44.19%) after 21 days. Fig. 3b showed the release kinetics of VEGF, FGF-2 and BMP-2 from the composite scaffold loaded with PLGA-PEG-COOH_{mp} and Gelatin_{mp} for three weeks. Within the first 7 days, cumulative release rates of FGF-2 and VEGF from the composite scaffold was 36.76% and 35.10%, which was significantly higher than that of BMP-2 (14.17%). After 21 days, cumulative release rates of FGF-2, VEGF and BMP-2 were about 49.65, 48.24 and 32.56%, respectively. These findings showed that the release rates of VEGF and FGF-2 from gelatin_{mp} were much faster than those of BMP-2 from PLGA-PEG-COOH_{mp} before the 7th day. VEGF and FGF-2 released from gelatin_{mp} was slightly faster than BMP-2 released from PLGA-PEG-COOH_{mp} after the 7th day. After 14 days, the release rates of VEGF and FGF-2 from gelatin_{mp} were slower than that of BMP-2 from PLGA-PEG-COOH_{mp}. These data suggested that the release rates of FGF-2 and VEGF

were much faster than those of BMP-2, and large amounts of VEGF and FGF-2 were released from the composite scaffold.

3.3. Effects of BMP-2-PLGA-PEG-COOH_{mp}/VEGF-FGF-2-gelatin_{mp}/nHA-PLGA scaffold on osteogenic differentiation of BMSCs *in vitro*

To investigate the effects of dual release of FGF-2, VEGF and BMP-2 on BMSCs proliferation and differentiation, BMSCs were randomized into four groups: (1) Control group (DMEM+ 10% FBS); (2) Free BMP-2+VEGF + FGF-2 (BMP-2, VEGF and FGF-2 were directly added into the culture medium); (3) Dual release of BMP-2, VEGF and FGF-2 from scaffold (BMP-2-PLGA-PEG-COOH_{mp}/VEGF-FGF-2-Gelatin_{mp}/nHA-PLGA scaffold); (4) Non-loaded nHA-PLGA scaffold (nHA-PLGA scaffold without growth factor). Fig. 4a shows the proliferation of BMSCs. After 7 days of culture, proliferations of BMSCs in the free growth factor solution and dual-released groups were significantly better than that those of the control and non-loaded nHA-PLGA scaffold groups ($p < 0.01$). Moreover, on days 14 and 21, the dual-released group exhibited higher levels of BMSCs proliferation relative to the other 3 groups. As shown in Fig. 4b and c, there were no significant differences in mRNA expression levels of osteogenic differentiation-related genes, including Col-I and OCN in BMSCs on 1 day. However, after 14 days, dual release of growth factors from the scaffold significantly elevated Col-I and OCN mRNA expression levels, especially on the 21st day ($p < 0.01$). These findings implied that dual delivery of growth factors could promote osteogenic differentiation of BMSCs.

To establish how the BMP-2-PLGA-PEG-COOH_{mp}/VEGF-FGF-2-Gelatin_{mp}/nHA-PLGA composite scaffold influences the growth of BMSCs, cell cycles were assessed by flow cytometry (Fig. 4d–h). The composite scaffold promoted the transition of cells from G0/G1 phase to S and G2/M phase. Cells abundance in the S and G2/M phases of the scaffold group were higher than those of the other experimental groups, implying an increased transition from G0 to S phases. Increased cell ratio in the S and G2/M phases indicated significant synergistic effects of growth factors on the cell cycle. The low abundance of G0/G1 resident BMSCs cultured with composite scaffolds as shown by the decrease in apoptosis and increase in cells in the division phase suggested that cell divisions was enhanced. Therefore, dual release of growth factors from the composite scaffolds significantly improved progression from the G1 to S phase, improved DNA replication and reduced apoptosis. This was attributed to growth factor deprivation, which stimulated cell cycle progression and proliferation.

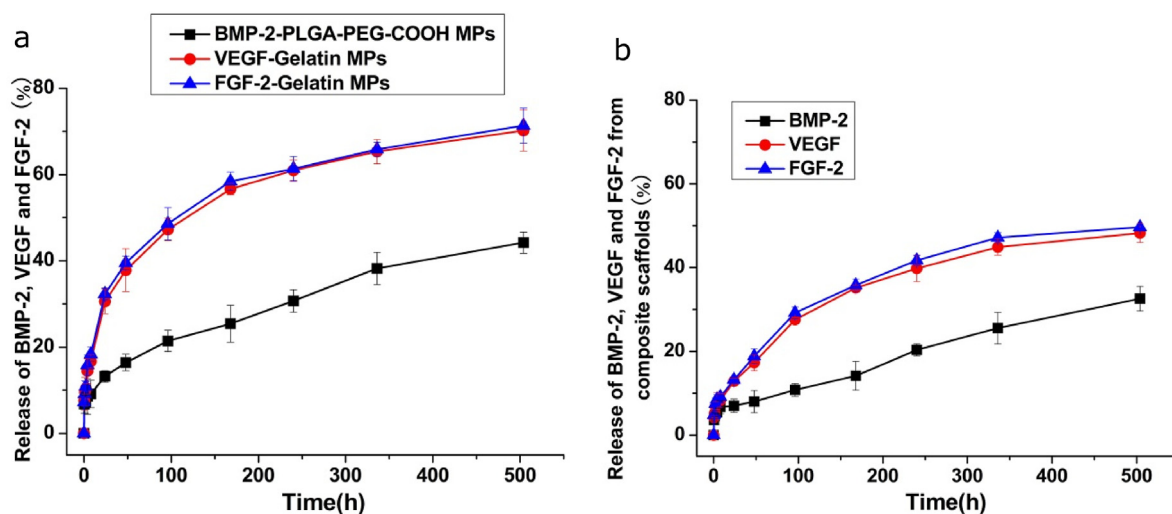


Figure 3. *In vitro* cumulative release of BMP-2 (black circles), VEGF (red circles) and FGF-2 (blue circles). (a) Release of BMP-2-loaded PLGA-PEG-COOH_{mp} and VEGF-FGF-2-loaded gelatin_{mp}. (b) Release of BMP-2-loaded PLGA-PEG-COOH_{mp} and VEGF-FGF-2-loaded gelatin_{mp} contained in nHA-PLGA scaffolds over three weeks period. Each value represents the mean \pm SD ($n = 3$).

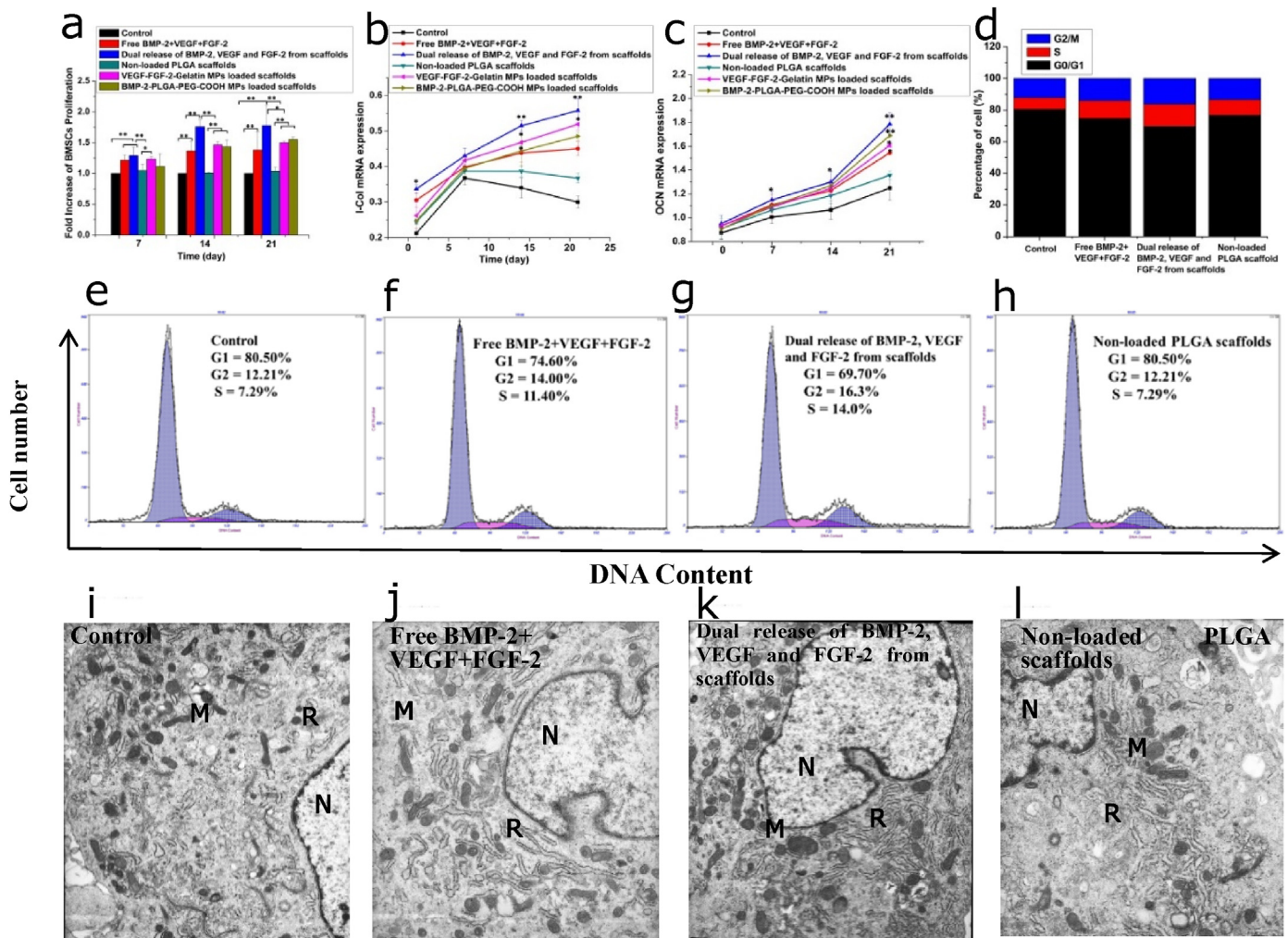


Figure 4. Effects of dual release of FGF-2, VEGF and BMP-2 from composite scaffolds on BMSCs proliferation and osteogenic differentiation. (a) BMSCs viability detected on the 7th, 14th and 21st day. (b) I-COL mRNA expression in BMSCs. (c) OCN mRNA expression in BMSCs. (d) Histogram distribution of cells in the G0/G1, S and G2/M phases (e–h) Cell cycle of BMSCs (i–l) TEM photographs of BMSCs with different treatments, N = nucleus; M = mitochondria; R = rough endoplasmic reticulum, × 8000. Each data point represents the mean ± standard deviation (n = 3), statistically significant differences are indicated as *p < 0.05 and **p < 0.01.

To investigate the effects of dual release of growth factors from the composite scaffold on the organelles of BMSCs, BMSCs ultrastructures were observed by transmission electron microscopy (Fig. 4i–l). As shown in Fig. 4i, BMSCs in the control group exhibited common stem cell characteristics, such as a clear nucleus and an abundant cytoplasm. There were a lot of organelles in the cytoplasm, including the mitochondria, rough endoplasmic reticulum and ribosomes. The nuclear membrane and nucleolus were clear, while chromatin was evenly distributed in the nucleus. BMSCs cultured in the free growth factor solution showed a high abundance of mitochondria and rough endoplasmic reticulum, relative to the control. Differentiated cell characteristics were also observed, including a thick nuclear membrane and decreased ratios of the nucleus and plasma. These characteristics implied cells were preparing for mitosis (Fig. 4j). As shown in Fig. 4k, BMSCs cultured with the composite scaffold showed obvious secretory cell morphologies. There were more significant secretory vesicles and a few white phagocytic vesicles in the cytoplasm, which proved that cells had higher secretory activities and stronger abilities for protein synthesis. Besides, the abundance of mitochondria and rough endoplasmic reticulum were significantly increased, indicating cell maturation and differentiation. As shown in TEM images of BMSCs cultured with non-loaded nHA-PLGA scaffolds, ultrastructures of BMSCs were comparable to those of the control group, and many secondary lysosomes were distributed in the cytoplasm (Fig. 4l). There-

fore, relative to the other groups, the composite scaffold with dual release of growth factors provided an ideal microenvironment for cell growth.

ALP staining was performed to investigate osteogenic differentiation of BMSCs cultured in different conditions. As shown in Fig. 5a, the control and non-loaded nHA-PLGA scaffold groups only showed faint ALP staining. Moreover, the dual released scaffold group exhibited stronger staining outcomes compared to the free BMP-2+VEGF + FGF-2 group. Quantitative detection of ALP activities were shown in Fig. 5c. After 7 days, ALP activities of BMSCs in the free growth factors solution and dual released growth factors group were significantly high than those of the other groups. Importantly, ALP activities were dramatically increased in the growth factors dual delivery group, compared to the other groups (p < 0.01). These findings proved that dual release of FGF-2, VEGF and BMP-2 induced higher ALP activities in BMSCs, relative to simultaneous single applications of the growth factors. Matrix mineralization abilities of BMSCs were detected by ARS staining. As shown in Fig. 5b, after 21 days of culture, ALP staining in the dual release of FGF-2, VEGF and BMP-2 from scaffold group was darker, relative to the other groups (p < 0.01). Quantitative analysis of ARS staining was consistent with these results (Fig. 5d), which showed significantly high calcium deposition in dual growth factors released scaffold group. These results indicated that BMSCs in the growth factor dual released scaffold group exhibited stronger osteogenic effects.

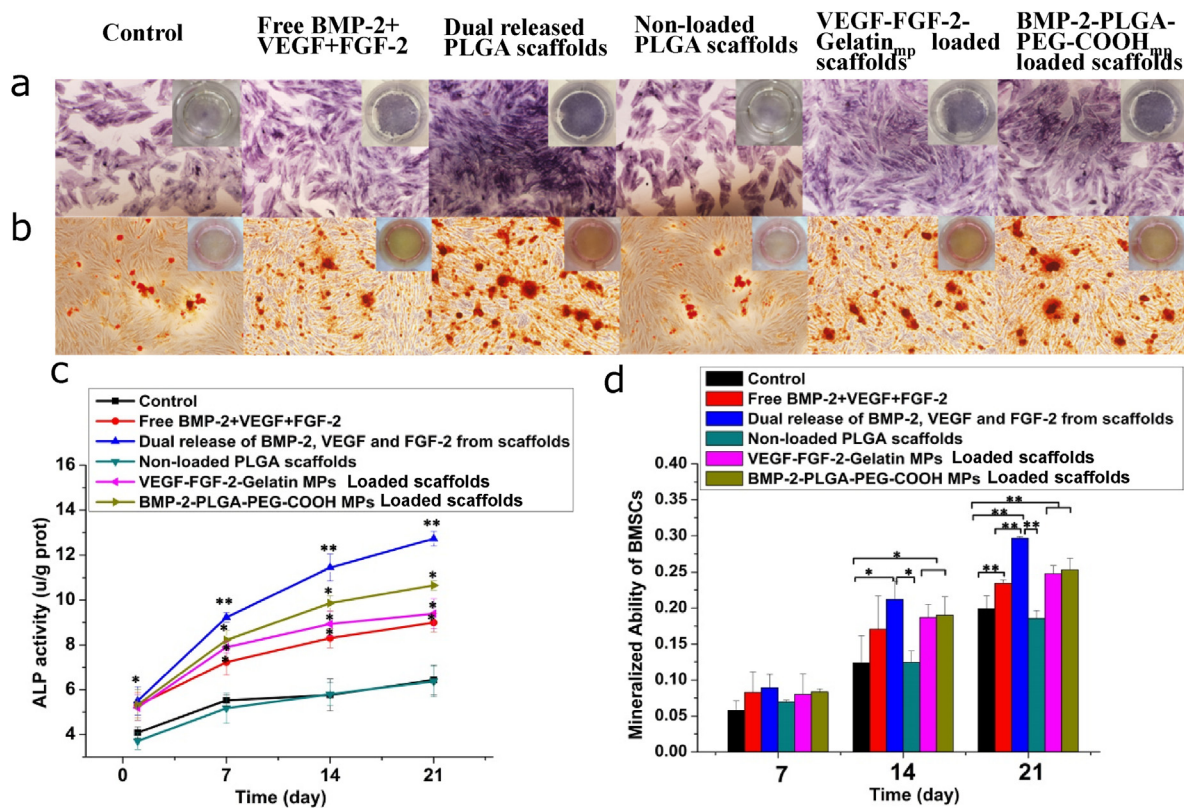


Figure 5. Effects of dual release of FGF-2, VEGF and BMP-2 from composite scaffolds on osteogenic differentiation of BMSCs. (a) ALP staining on the 7th day. (b) Alizarin red S staining on the 21st day. (c) ALP activity determined by colorimetry using ALP kit. (d) Mineralized ability of BMSCs based on the results of Alizarin red S staining. Each data point represents the mean \pm standard deviation ($n = 3$), statistically significant differences are indicated as * $p < 0.05$ and ** $p < 0.01$.

3.4. Effects of the BMP-2-PLGA-PEG-COOH_{mp}/VEGF-FGF-2-gelatin_{mp}/nHA-PLGA composite scaffold on functional connection of osteoblast-vascular cells in the co-culture system

As shown in Fig. 6a, composite scaffolds seeded with BMSCs were incubated in the upper chamber, while HUVECs were implanted in the lower chamber of the transwell plate to determine if the effects of dual release of growth factors on BMSCs had any effects on HUVECs proliferation and differentiation. The proliferation of HUVECs was shown in Fig. 6b. HUVECs cultured with the BMP-2-PLGA-PEG-COOH_{mp}/VEGF-FGF-2-Gelatin_{mp}/nHA-PLGA composite scaffold exhibited enhanced cell proliferation rates. These results demonstrated that the dual release of growth factors from scaffolds could stimulate HUVECs proliferation. Proliferation rates of HUVECs co-cultured with BMSCs seeded on composite scaffolds were significantly enhanced compared to those of HUVECs co-cultured with non-loaded scaffolds and composite scaffolds without BMSCs. Then, expression levels of typical HUVECs differentiation-related genes were evaluated by qRT-PCR on the 14th day. As shown in Fig. 6c, HUVECs co-cultured with composite scaffolds exhibited higher mRNA expression levels of angiogenic genes, relative to those co-cultured with non-loaded scaffolds. Moreover, expression levels of the differentiation-related genes in HUVECs co-cultured with BMSCs seeded on the composite scaffolds were improved compared to those of composite scaffolds without BMSCs. These results were consistent with those of MMP-2 and MMP-9 levels (Fig. 6d). HUVECs co-cultured with composite scaffolds and BMSCs exhibited higher levels of MMP-2 and MMP-9, relative to those cultured with the composite scaffold alone. These findings suggested that BMSCs seeded on the BMP-2-PLGA-PEG-COOH_{mp}/VEGF-FGF-2-Gelatin_{mp}/nHA-PLGA composite scaffold

promoted the expression of differentiation related genes and proteins in HUVECs.

ECs migration is an important event in angiogenesis, which involves the regeneration of new blood vessels. Therefore, we investigated the effects of dual release of FGF-2, VEGF and BMP-2 from composite scaffolds on the migration of HUVECs co-cultured with BMSCs. As shown in Fig. 7a and c, dual release of growth factors from the scaffold enhanced HUVECs migration compared to the non-loaded scaffold. The composite scaffold, seeded with BMSCs, improved the migration of HUVECs, compared to the scaffold without BMSCs. Notably, the BMSC-seeded scaffold exerted significant effects on migration, which significantly improved the “wound healing” effects. Subsequently, we determined if the composite scaffold seeded with BMSCs could enhance tube formation in HUVECs. Tubular structure formation by HUVECs co-cultures with different scaffold groups was assessed on the 7th days. As shown in Fig. 7b and d, HUVECs co-incubated with BMSCs and non-loaded PLGA scaffolds exhibited limited tubular structures and branching points, while HUVECs co-incubated with BMSCs and dual delivery scaffolds formed many tubular structures as well as branching points. Besides, the formation of tubular structures in the dual delivery scaffolds was significantly better than those of non-loaded PLGA scaffolds. These results confirm that dual release of multiple growth factors from the composite scaffold promoted lumen formation abilities of HUVECs in the co-culture system.

Angiogenesis involves the migration of endothelial cells across the basement membrane and into the perivascular matrix. Therefore, invasion abilities of HUVECs were investigated. The non-contracting co-culture system was established as shown in Fig. 8a. To determine if the effects of dual delivery scaffold on BMSCs further promoted HUVECs

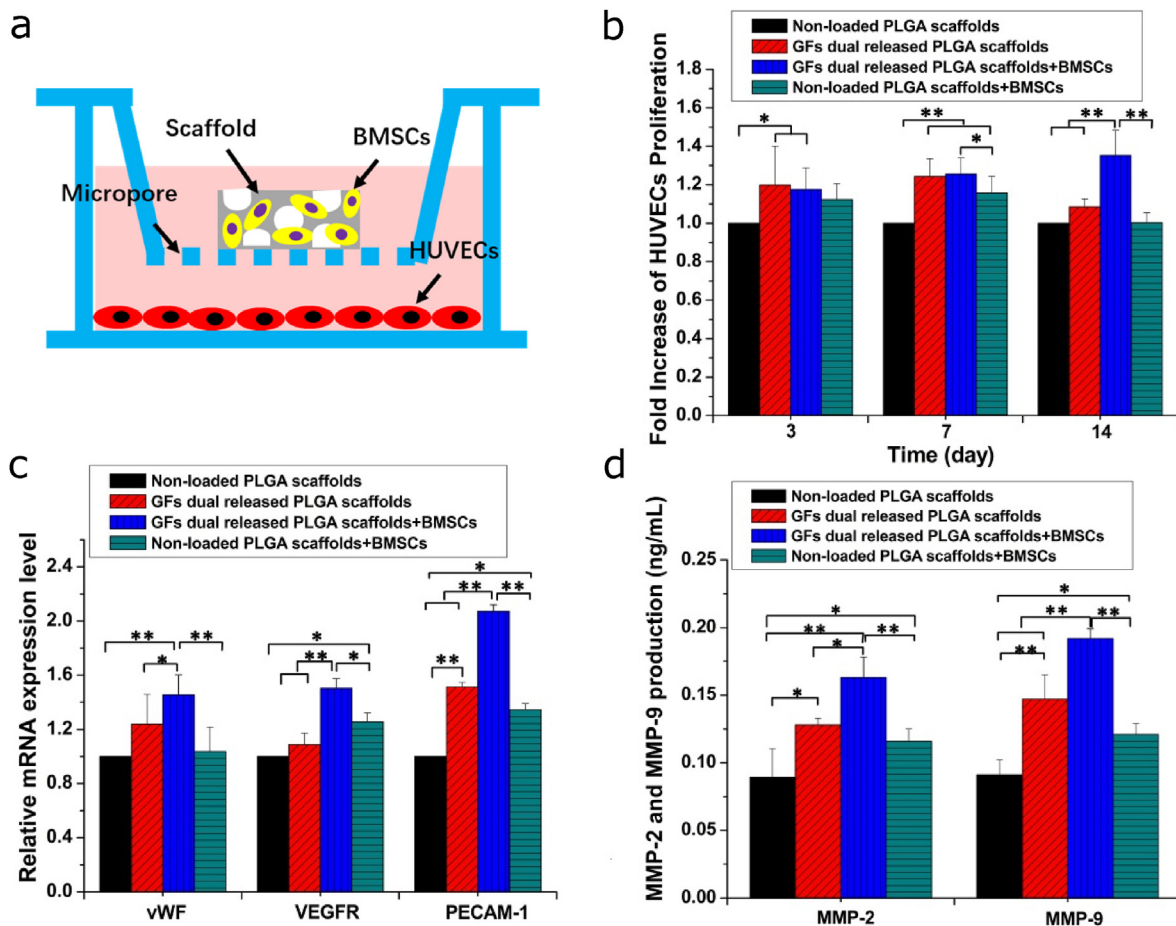


Figure 6. Proliferation and differentiation of HUVECs co-cultured with scaffolds seeded with BMSCs. (a) Scheme for the structure of non-contacting co-culture system. (b) Proliferation of HUVECs on 3rd, 7th and 14th days. (c) Angiogenic differentiation genes expression of HUVECs. (d) Quantitative analysis of MMP-2 and MMP-9. Each data point represents the mean \pm standard deviation ($n = 3$), statistically significant differences are indicated as * $p < 0.05$ and ** $p < 0.01$.

invasion, HUVECs were cultured in the apical compartment, while the scaffold seeded with BMSCs was cultured in the basolateral compartment. As shown in Fig. 8b and c, composite scaffolds markedly promoted HUVECs invasion, relative to the non-loaded PLGA scaffolds ($p < 0.01$), while composite scaffolds seeded with BMSCs significantly improved invasion compared to composite scaffolds without BMSCs. Dual growth factors released from the composite scaffold enhanced the invasion of HUVECs compared with other groups ($p < 0.01$).

3.5. Effects of BMP-2-PLGA-PEG-COOH_{mp}/VEGF-FGF-2-gelatin_{mp}/nHA-PLGA composite scaffold on angiogenic growth factors paracrine of BMSCs

Since BMSCs and HUVECs were co-cultured in a non-contact manner, stimulation of HUVECs differentiation was probably due to composite scaffolds inducing BMSCs to secrete angiogenic factors. Besides, BMSCs secreted most of the cytokines required for angiogenesis when they were cultured alone [32]. To investigate this hypothesis, gene expressions of some growth factors were tested by qRT-PCR. As shown in Fig. 9a, mRNA expression levels of TIMP-1, Ang-1 and HGF were low, therefore, they were not detected. Theoretically, it has been shown that BMSCs can secrete these factors, therefore, all angiogenic factors should be detectable [32]. The low expression levels of these growth factor genes were attributed to two factors. First, BMSCs used in previous studies and in this study were derived from different species, and gene expression levels have been shown to greatly vary among species. Second, cell culture conditions could have effects on mRNA expression. In this study, mRNA

expression levels of IGF, IL-6 and VEGF in BMSCs cultured with the composite scaffold were higher than those of the other groups. Commercial ELISA kits were used to assess proteins levels of the growth factors (Fig. 9b). Even though protein levels of IL-6 and IGF in BMSCs cultured with composite scaffolds were elevated compared to those cultured with other groups, differences were not significant. Moreover, protein levels of VEGF in BMSCs cultured on composite scaffolds were significantly elevated. These results proved that the enhanced HUVECs growth and differentiation may be because of increased VEGF expressions by BMSCs cultured with composite scaffolds. To further verify this conclusion, JK-P3 was used as an inhibitor to block the VEGF receptor [33], after which the proliferation and differentiation levels of HUVECs were evaluated. We found that the inhibitor suppressed the proliferation and differentiation of HUVECs cultured in the composite scaffolds and nHA-PLGA scaffolds (Fig. 9c and d), which further confirmed that elevated expression of VEGF in BMSCs seeded in the composite scaffold was the main reason for the increased proliferation and differentiation of HUVECs.

3.6. New bone and blood vessel formation in femur defects with implanted scaffolds

Twelve weeks after implantation, micro-CT analysis was performed to analyze new bone formation in defect sites where scaffolds had been implanted. Fig. 10a showed the position of the bone tunnel and new bone formation in the four groups. The B-PPC_{mp}/VF-GEL_{mp}/nHA-PLGA scaffold

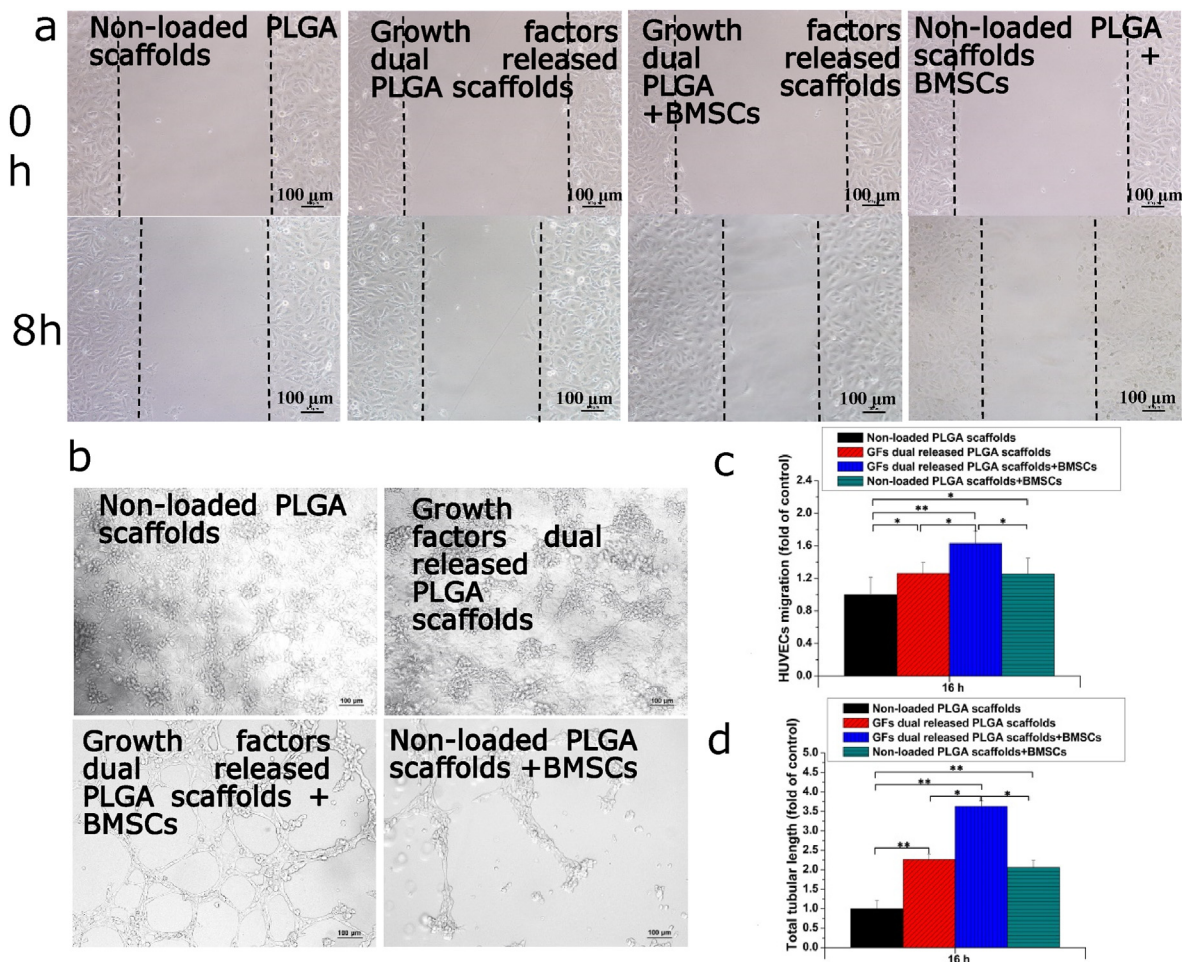


Figure 7. Migration and Tube formation of HUVECs co-cultured with BMSCs seeded in scaffolds. (a) Closure of the wound healing. (b) The capillary-like tube formation. (c) The distance of HUVECs migration. (d) The total tubular length. Each data point represents the mean \pm standard deviation ($n = 3$), statistically-significant differences are indicated as * $p < 0.05$ and ** $p < 0.01$. Scale bar 100 μ m.

fold group had more bone formation, compared to the nHA-PLGA scaffold, BVF/nHA-PLGA scaffold and the unfilled defect groups at 12 weeks post-surgery. The three-dimensional (3D) reconstructed images were showed in Fig. 10b. The unfilled defect group exhibited poorly regenerated femurs, indicating a limited self-healing capacity. New bone formation in the nHA-PLGA scaffold and BVF/nHA-PLGA scaffold groups were better than those of the unfilled defect group. Importantly, the group implanted with B-PPC_{mp}/VF-GEL_{mp}/nHA-PLGA scaffolds exhibited higher bone mineral densities compared to other groups. As shown in 3D images of reconstructed bone defect tunnel (Fig. 10c), new bone formation in the B-PPC_{mp}/VF-GEL_{mp}/nHA-PLGA scaffold group was higher, compared to other groups.

To evaluate osteogenesis within the scaffolds, a region with a height of 3 mm and a diameter of 2.5 mm was selected for quantitative assessments (Fig. 10d). Based on 3D images, the BVF/nHA-PLGA scaffold group was associated with elevated BV/TV, BMD, Tb.Th, and Tb.N levels and suppressed Tb. Sp levels, relative to the unfilled defect group ($p < 0.0001$) and the nHA-PLGA scaffold group ($p < 0.01$). Moreover, the B-PPC_{mp}/VF-GEL_{mp}/nHA-PLGA scaffold group exhibited significantly high BMD, BV/TV, Tb.N, and Tb.Th levels and suppressed Tb. Sp levels, when compared to the nHA-PLGA scaffold ($p < 0.0001$). Compared to the BVF/nHA-PLGA scaffold group, significantly elevated BMD (0.91 g/cm³, $p < 0.01$), BV/TV (46.92%, $p < 0.01$), Tb.Th (0.226 mm, $p < 0.01$), Tb.N (3.45/mm, $p < 0.001$) and significantly suppressed Tb. Sp (0.21 mm, $p < 0.0001$) levels were noted in the B-PPC_{mp}/VF-GEL_{mp}/nHA-PLGA scaffold group.

To investigate bone formation inside the porous scaffolds, middle cross sections of defects were analyzed by histological and immunohistochemical evaluation (Fig. 11). Immature Masson trichrome staining of bone tissues in the spaces of scaffolds was light blue. At 12 weeks post-surgery, some new islands of bone tissues were observed in the degraded nHA-PLGA scaffold, BVF/nHA-PLGA and B-PPC_{mp}/VF-GEL_{mp}/nHA-PLGA scaffolds, whereas defect zones of the control group were full of fibrous connective tissues. More new bone tissues in the defects were formed in the B-PPC_{mp}/VF-GEL_{mp}/nHA-PLGA scaffold group than other groups, and scaffolds residues were integrated with the surrounding tissues. This finding suggested that the B-PPC_{mp}/VF-GEL_{mp}/nHA-PLGA scaffold promoted bone regeneration. Immunohistochemical staining of CD31 showed that it was widely distributed in the new formed tissues. The abundance of new generated blood vessels with CD31-positive cells in the B-PPC_{mp}/VF-GEL_{mp}/nHA-PLGA scaffold group was significantly high, compared to the other groups. High vascularization levels in the B-PPC_{mp}/VF-GEL_{mp}/nHA-PLGA scaffold group indicated that dual delivery of FGF-2, VEGF and BMP-2 from the composite scaffold enhanced angiogenesis during bone regeneration.

4. Discussion

Clinically, the reconstruction of bone defects caused by trauma, infection and tumors is challenging. Bone repair is a complex and precisely regulated process, involving many effective factors, such as growth factors and physiological conditions among others. Coordination of

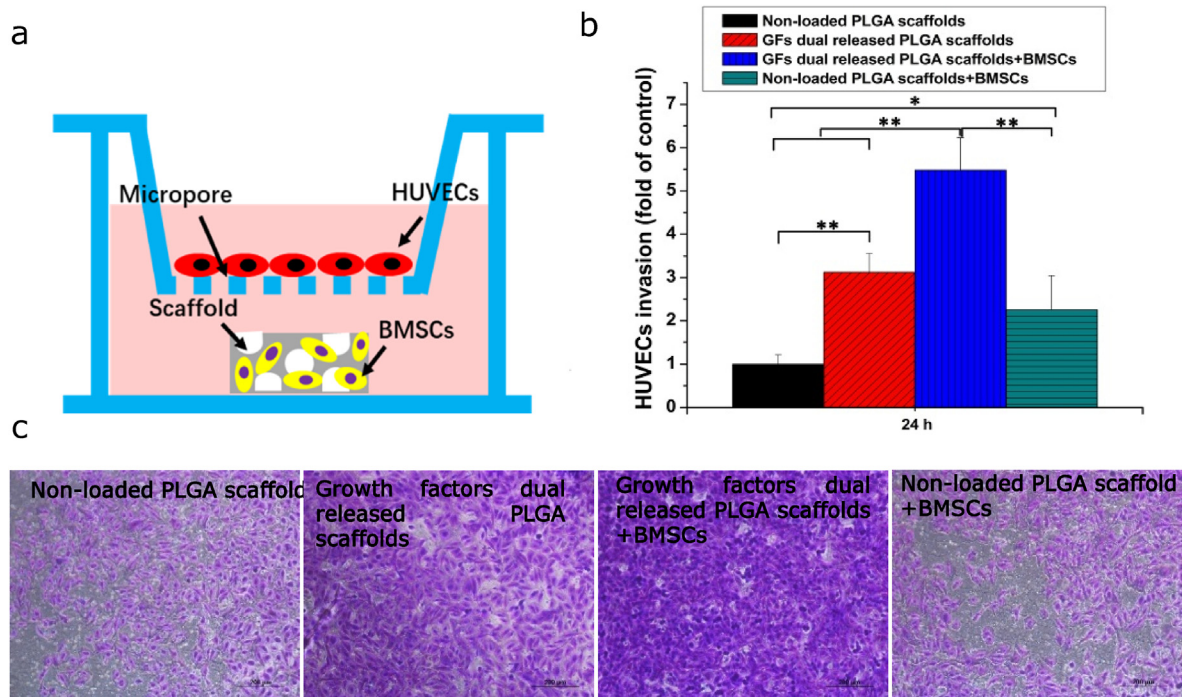


Figure 8. Invasion of HUVECs co-cultured with scaffolds seeded with BMSCs. (a) Scheme for the structure of non-contacting co-culture system. (b) Extracted crystal violet of invaded cells. (c) The number of HUVECs invasion. Each data point represents the mean \pm standard deviation ($n = 3$), statistically significant differences are indicated as $*p < 0.05$ and $**p < 0.01$. Scale bar 200 μm .

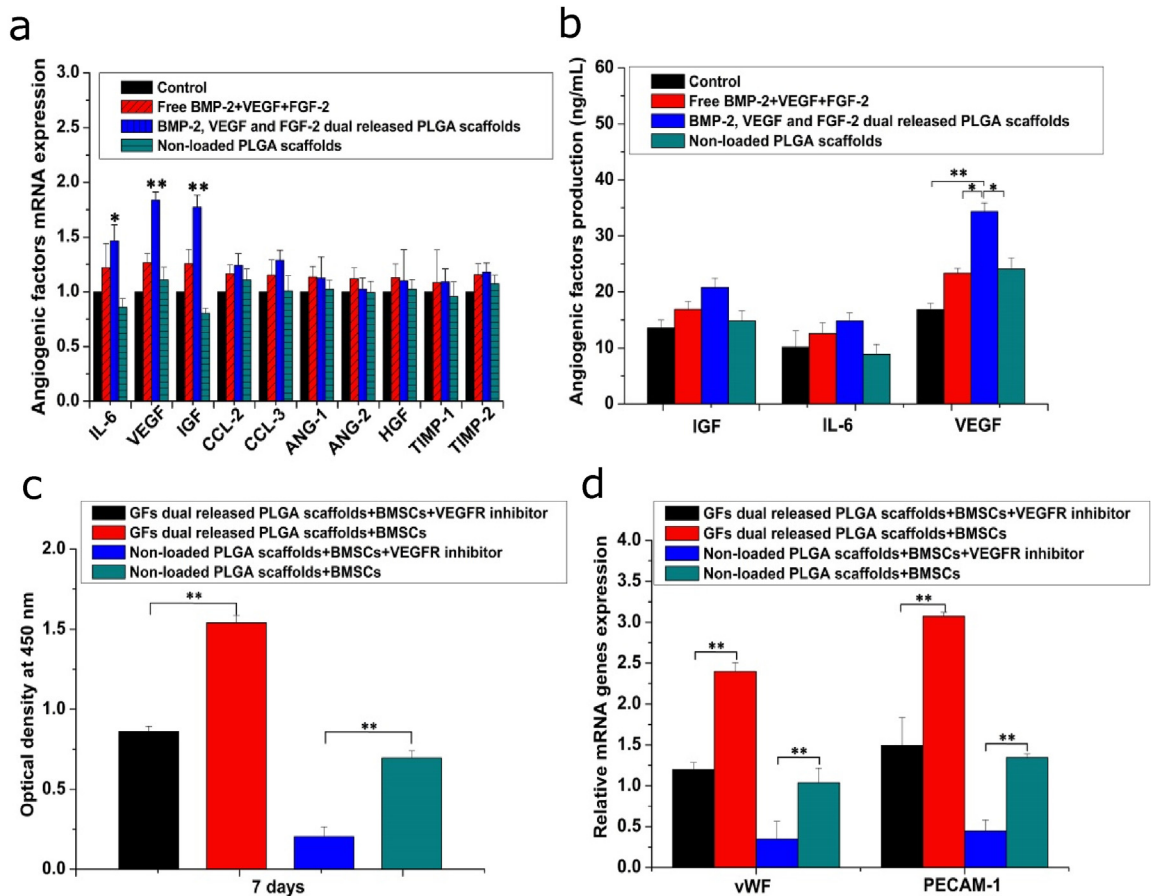


Figure 9. Effects of dual release of BMP-2, VEGF and FGF-2 on angiogenic factors paracrine. (a) Angiogenic factors expression in BMSCs on the 7th day. (b) Quantitative analysis of angiogenic factors expression. (c) HUVECs proliferation after blocking VEGFR using JK-P3 as inhibitor. (d) Angiogenic differentiation-related proteins secretion after blocking VEGFR. Each data point represents the mean \pm standard deviation ($n = 3$), statistically significant differences are indicated as $*p < 0.05$ and $**p < 0.01$.

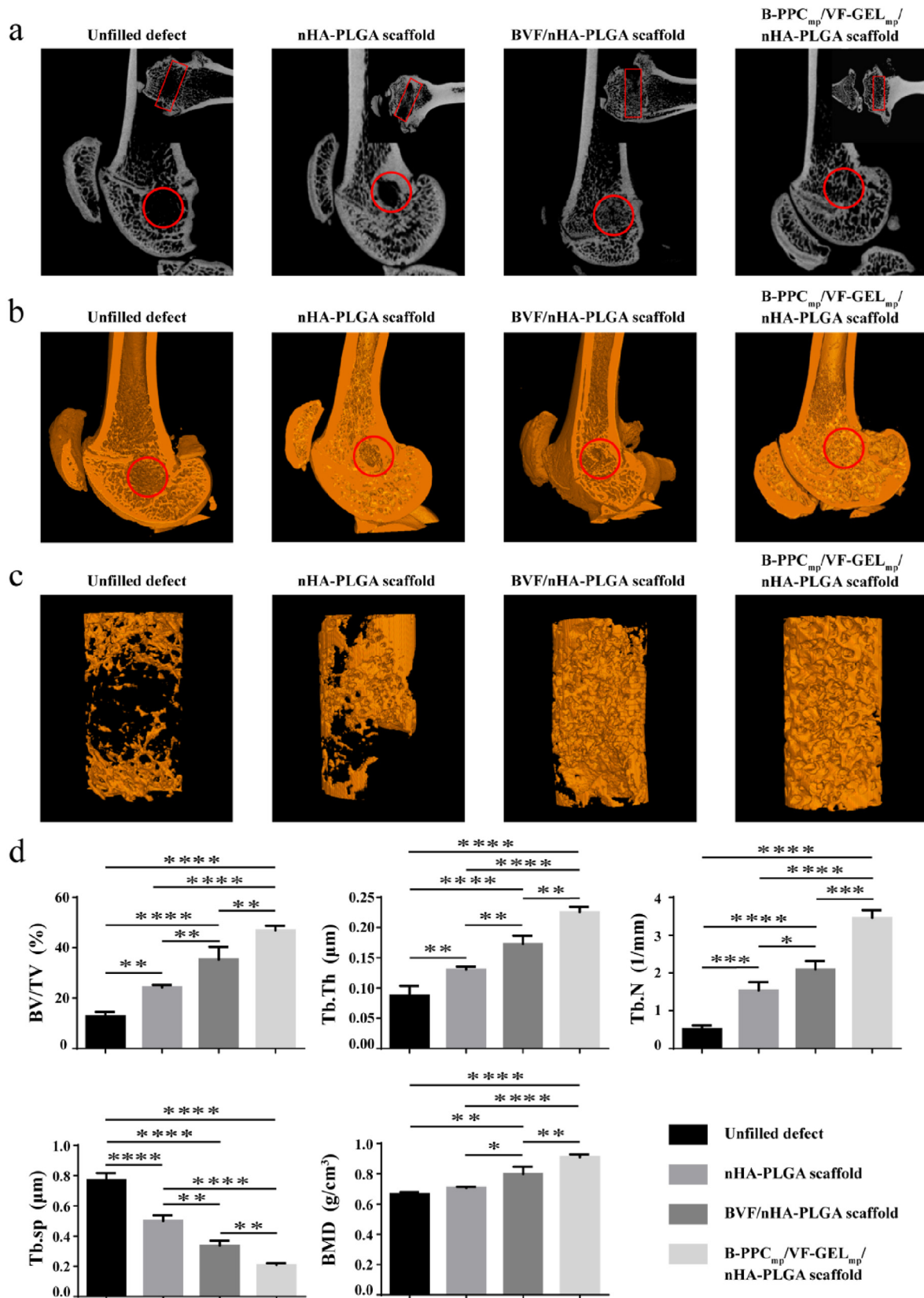


Figure 10. New bone formation within the femur defects at 12 weeks post-surgery. (a) 2D micro-CT images of implantation area. The circles indicate sagittal plane, rectangles indicate coronal plane. (b) 3D micro-CT images of mineralized bone formation. The circles indicate the original defect areas. (c) 3D micro-CT reconstruction images of implant areas. Orange regions indicate new bone. (d) Quantitative analysis of micro-CT of bone regeneration. Bone volume fractions (BV/TV), trabecular thickness (Tb.Th), trabecular number (Tb.N), trabecular spacing (Tb.Sp), bone mineral density (BMD). Each data point represents the mean ± standard deviation (n = 3), statistically significant differences are indicated as * P < 0.05, **P < 0.01, ***P < 0.001, ****P < 0.0001.

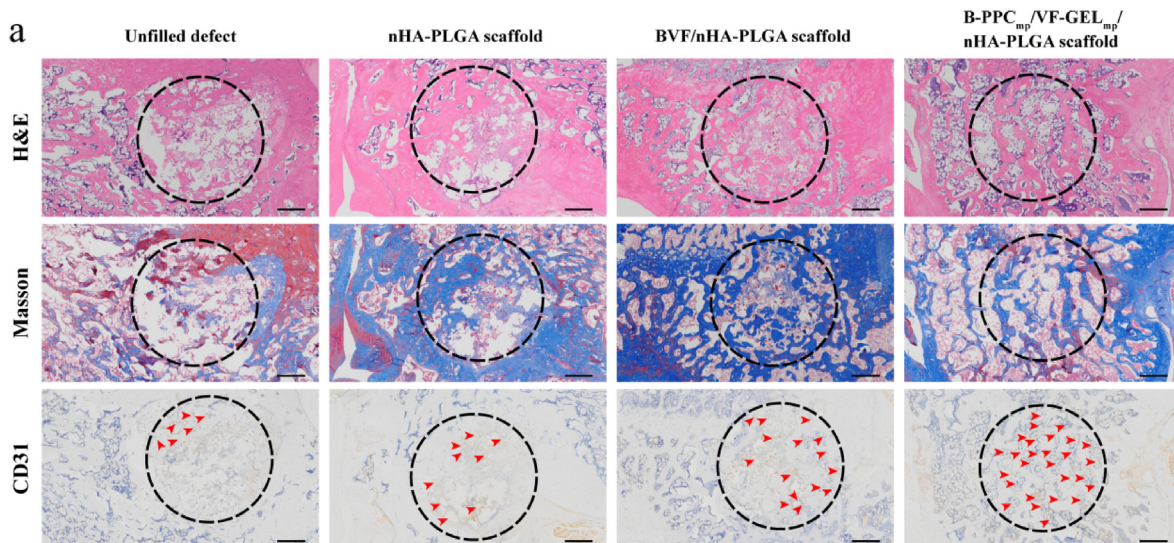


Figure 11. Histological and immunohistochemical analysis (H&E, Masson's trichrome and CD31) of the cavity defects in lateral femoral condyle. The dashed-line circles indicate the original defect areas. Red arrowheads indicate the newly formed blood vessels. Scale bars: 500 μm .

growth and differentiation of seeded cells as well as the release of growth factors and scaffolds is key in bone defect regeneration. To improve bone regeneration by promoting osteogenic differentiation of osteoprogenitor cells and angiogenesis of endothelial cells, we developed a dual growth factor delivery system to simulate the bone regeneration environment. In this study, we designed and developed a novel composite scaffold that could specifically deliver different growth factors to damaged tissues at different doses and rates. These results indicated that femur regeneration was significantly promoted by time-dynamic release of critical growth factors from the composite scaffold and their stimulation on osteoblast-vascular cell communication during bone formation. Controlled release of these growth factors *in situ* from biodegradable scaffolds with different kinetic rates can ultimately promote the regeneration of damaged tissue.

We developed a composite scaffold with the capacity for controlled release of osteogenic and angiogenic growth factors to enhance vascularization and bone regeneration. Given that BMP-2 expressions occurred during the whole process of fracture healing, while VEGF and FGF-2 were only expressed in the early stages (strongly detected in 5–10 days) [34–36], BMP-2 was loaded into PLGA-PEG-COOH_{mp} via the self-assembly technique to prolong the release period. Meanwhile, FGF-2 and VEGF were packed into Gelatin_{mp} through the entrapment technique to obtain a relatively fast release than BMP-2. Encapsulation of growth factors into microparticles maintained their biological activities, and controlled their release rates. To realize this design, the supercritical CO₂ foaming technique was used to encapsulate BMP-2-PLGA-PEG-COOH_{mp} and VEGF-FGF-2-Gelatin_{mp} into nHA-PLGA composite scaffolds, thereby, fabricating a composite BMP-2-PLGA-PEG-COOH_{mp}/VEGF-FGF-2-Gelatin_{mp}/nHA-PLGA scaffold. We found that over 21 days, cumulative release of FGF-2 and VEGF from Gelatin_{mp} was markedly high than that of BMP-2 from BMP-2-PLGA-PEG-COOH_{mp} ($p < 0.05$). Moreover, the encapsulation of microparticles into nHA-PLGA-based scaffolds sustained the release rate, which met the repair needs. Compared to the slow-degrading PLGA-PEG-COOH_{mp}, rapid degradation of Gelatin_{mp} led to a faster release rate. The dual release of FGF-2 and VEGF followed by BMP-2 was achieved by loading both FGF-2 and VEGF into Gelatin_{mp}, and BMP-2 into PLGA-PEG-COOH_{mp} (Fig. 12a). Thus, by modeling the expression sequence of these growth factors during fracture repair, they exerted synergistic effects on cell differentiation and tissue regeneration. Fig. 3a and b showed that the presence of BMP-2-PLGA-PEG-COOH_{mp} within the scaffolds had no effect on the release of VEGF-FGF-2-Gelatin_{mp}. One of the advantages of our dual delivery system is that the release rate of each growth factor could be separately regulated by

changing material properties and preparation parameters of Gelatin_{mp} and PLGA-PEG-COOH_{mp} respectively. For instance, the release of growth factors could be regulated by selecting the molecular weight or lactide to glycolide ratio of PLGA-PEG-COOH_{mp}, and through different chemistries to control the fabrication processes of Gelatin_{mp} microparticles. The ability of the composite scaffolds to control the release of different growth factors at distinct rates was investigated. These scaffolds provide a viable strategy for investigating various important regeneration and development processes in biology.

Our results confirmed that the dually released growth factors from composite scaffolds maintained their bioactivities after 3 weeks and subsequently, stimulated osteogenic differentiation of BMSCs. VEGF and FGF-2 were rapidly released from composite scaffolds to promote BMSCs proliferation, meanwhile, BMP-2 was deliberately released to promote BMSCs differentiation into osteoblasts, thereby enhancing their mineralization. In our previous studies, VEGF, FGF-2 and BMP-2 were found to play different regulatory roles in the process of BMSCs differentiation. They exerted synergistic effects on cell proliferation and differentiation in a time-dependent manner [2]. The dual delivery scaffold was shown to realize precise functions and synergistic effects of these growth factors. On one hand, VEGF is an early chemo-attractant for BMSCs, which enhances their recruitment, thereby promoting bone formation [37]. Besides, FGF-2 plays distinct biological functions during the osteogenic differentiation of BMSCs. It enhances the proliferation rate in the early stages and suppresses osteogenic differentiation as well as mature mineralization in the late stage [38]. Therefore, fast delivery of FGF-2 and VEGF stimulated cell proliferation, which was competent for osteogenic differentiation. During the early proliferation stage, VEGF and FGF-2 promote the expressions of BMP-2 receptors on cell surfaces [39], thereby enhancing the binding abilities of BMP-2 released in the later stages. Besides, the controlled release of BMP-2 is required for critical sized bone defects [40]. The burst and sustained release of BMP is necessary for the repair of bone defects. Since the burst of BMP-2 enhances the recruitment of osteoprogenitor cells into defect areas and increase the number of aggregate cells, the sustained release of BMP-2 promotes osteogenic differentiation of aggregate cells [41–43]. Moreover, our previous studies confirmed the synergistic effects of VEGF, FGF-2 and BMP-2 on osteogenic differentiation of BMSCs (Fig. 12b) [16]. VEGF/VEGFR interactions promote cell proliferation and downstream gene expressions through the MAPK/ERK signaling pathway [44,45]. FGF-2 promote cell proliferation and gene expressions of VEGF, BMP-2/BMP-2R and Runx2 by activating the MAPK/ERK signaling

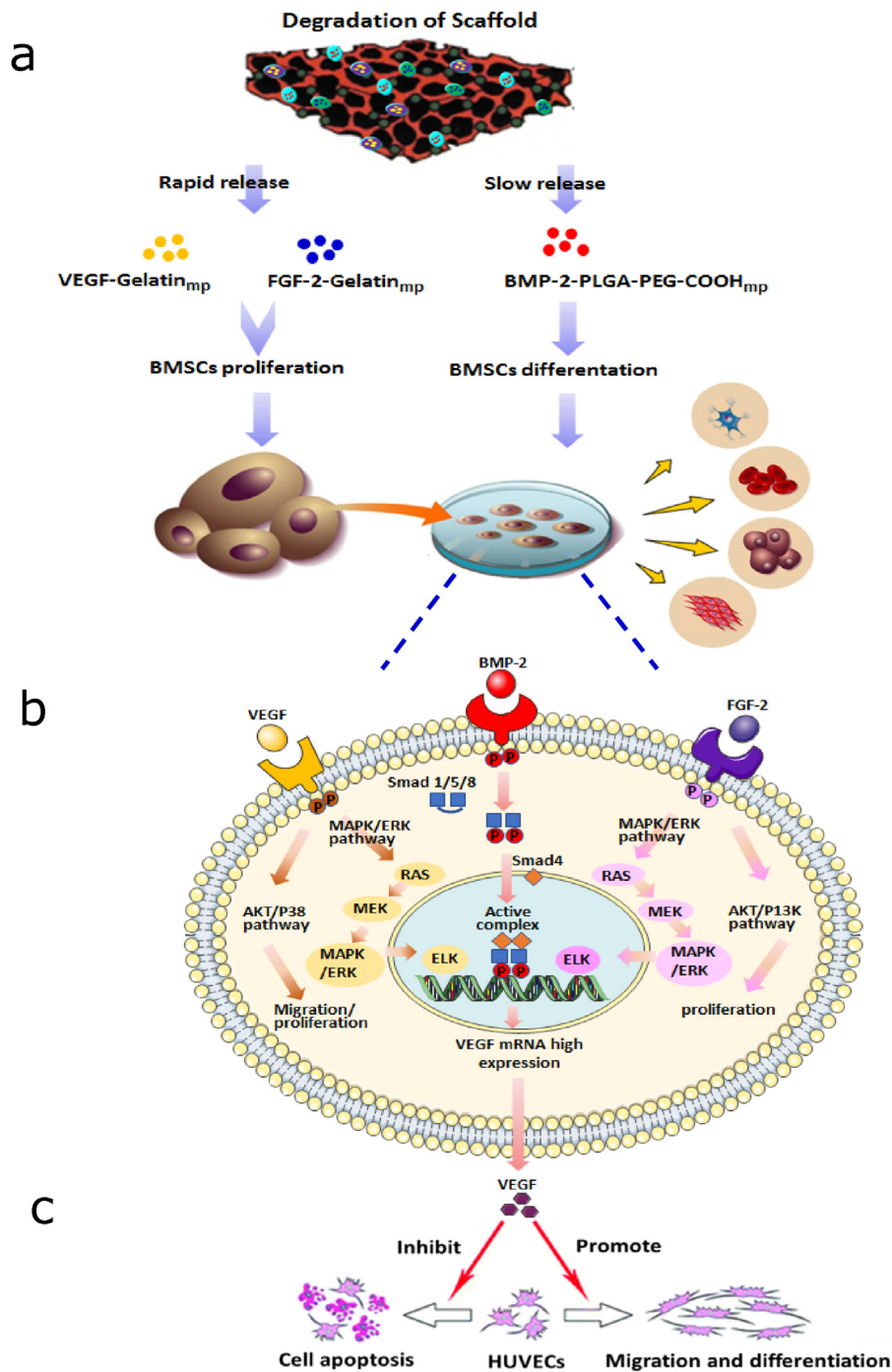


Figure 12. Scheme illustrates the mechanism of dual delivery of BMP-2, VEGF and FGF-2 from the composite scaffolds enhancing bone and blood vessel formation. (a) Dual release of VEGF and FGF-2 followed by BMP-2 was achieved by loading VEGF and FGF-2 into gelatin_{mp} and BMP-2 into PLGAPEG- COOH_{mp}. (b) The synergistic effects of VEGF, FGF- 2 and BMP-2 on BMSCs differentiation. (c) The functional connections of BMSCs-HUVECs were stimulated by secretion of VEGF from BMSCs.

pathway [46,47]. BMP-2/BMP-2R interactions activate phosphorylated Smad 1, 5 and 8 to form a heteromeric complex with Smad4 in the cytoplasm, which is then translocated into the nucleus to regulate the expressions of VEGF, FGF-2, Runx2/Cbfa 1 and other genes [48,49]. Complex interactions among FGF-2, VEGF and BMP can be achieved by regulating their respective signaling pathways, which significantly promotes BMSCs differentiation. Therefore, the dual delivery scaffold markedly accelerated the *in vitro* osteogenic differentiation cascade of BMSCs by realizing synergistic actions of VEGF, FGF-2 and BMP-2, which resulted in high osteogenic activities and abundant bone matrix formation.

Angiogenesis is important in bone development, remodeling and repair [50]. Angiogenesis provides nutrients for bone repair and helps in the recruitment of osteoprogenitor cells. The special populations of cells in blood vessels, known as endothelial cells, can also secrete cytokines that promote the differentiation of osteoprogenitor cells for bone repair [51]. Co-cultures of EPCs and BMSCs were shown to be beneficial to neo-vascularization [52,53]. Hence, we established a non-contact co-culture system to investigate communication between BMSCs and HUVECs. The HUVECs that had been co-cultured with BMSCs on BMP-2-PLGA-PEG-COOH_{mp}/VEGF-FGF-2-Gelatin_{mp}/nHA-PLGA scaffolds showed significantly increased cell viabilities, angiogenic differentiations and

capillary-like structure formation. Co-culture experiments showed that BMSCs seeded on composite scaffolds had the ability to modulate the proliferation and differentiation of HUVECs. The mechanism through which BMP-2-PLGA-PEG-COOH_{mp}/VEGF-FGF-2-Gelatin_{mp}/nHA-PLGA scaffolds regulate cell communication between BMSCs and HUVECs are shown in Fig. 12c. The synergistic effects of multiple growth factors from the composite scaffolds promote the expressions of VEGF, and enhance VEGF paracrine in the defect site, which improves HUVECs proliferation, differentiation, and tubular structure formation. Previously, communication and functional connection of osteoblast-vascular cells during bone development was found to be stimulated by localized secretion of paracrine signaling factors, such as VEGF and BMP-2 [53–55]. In accordance with this study, our dual delivery system stimulated the BMSCs-secreted VEGF, which promoted the proliferation and angiogenic differentiation of HUVECs. Therefore, the dual delivery system of growth factors plays a critical role in cell interactions during angiogenesis and bone repair. On one hand, dual delivery system recruits vascular endothelial cells and promotes angiogenic differentiation as well as new blood vessels formation. On the other hand, it recruits BMSCs and promotes their proliferation and osteogenic differentiation.

In vitro, compared to NHA-PLGA scaffolds, composite scaffolds released FGF-2, VEGF and BMP-2 at different rates, which exerted better effects on bone defects repair. Moreover, comparisons of bone repair between the BMP-2-PLGA-PEG-COOH_{mp}/VEGF-FGF-2-Gelatin_{mp}/nHA-PLGA scaffold group and MP-2/VEGF/FGF-2/nHA-PLGA scaffold group, revealed that implantation of dual growth factor delivery scaffolds in femoral defects markedly improved bone regeneration capacities. After 12 weeks, analyses of micro-CT and histological staining data revealed, more newly formed bone in the BMP-2-PLGA-PEG-COOH_{mp}/VEGF-FGF-2-Gelatin_{mp}/nHA-PLGA scaffold group. Through time course observation after implantation, the new bone was gradually integrated to replace the scaffolds. In addition, more blood vessels were formed in the composite scaffold group. The healing process of bone defects could be divided into three overlapping stages, scaffold degradation, angiogenesis and bone reconstruction [56]. In this process, high blood perfusion means more nutrition for the new bone growth in defect areas. Consistent with micro-CT results, more blood vessels resulted in an enhanced bone formation in the composite scaffold group. These findings confirmed that the BMP-2-PLGA-PEG-COOH_{mp}/VEGF-FGF-2-Gelatin_{mp}/nHA-PLGA scaffold accelerated cell differentiation, regulated functional connection of osteoblast-vascular cells, and promoted new bone as well as blood vessel formation in femur defects. Delivery of critical osteogenic and angiogenic growth factors at specific release rates through intelligent biodegradable scaffolds offered strategy for promoting bone defects repair. Therefore, polymeric scaffolds that regulate the precise, sustained and local release of various growth factors can be used to simulate temporal sequences of growth factor expression during natural bone formation. These results showed that loading FGF-2, VEGF and BMP-2 into a porous, biocompatible scaffold could ensure their precise delivery and efficient release into bone defects, which enhanced the formation of new bone tissues and blood vessels.

5. Conclusions

Sequential delivery of osteogenic and angiogenic growth factors by biodegradable composite scaffolds at different kinetic rates promoted the repair mechanisms of bone defects by mimicking *in vivo* environments of bone regeneration. Strategies to enable the sustained and coordinated release of multiple factors such as FGF-2, VEGF and BMP-2 from composite scaffolds provide a strategy for mimicking, at least partly, conditions in repair sequences of bone defects. We confirmed that the dual growth factor release system stimulated the communication and functional connection of osteoblast-vascular cells during bone development by promoting localized secretion of paracrine signaling factors in the co-culture system. The Gelatin and PLGA-PEG-COOH microparticle-based composite bioscaffolds exerted an osteogenic-angiogenic coupling effect

on bone regeneration, which provides a promising therapeutic approach for treatment of bone defects. Moreover, they can be used as models for studying interactions between seed cells, signaling factors and scaffold materials in tissue engineering.

Declaration of competing interest

The authors declared that we have no conflicts of interest to this work. We declare that we do not have any commercial or associative interest that represents a conflict of interest in connection with the work submitted.

Acknowledgements

This study was supported by the National Natural Science Foundation of China (81401535), Discipline talents development projects of School of Pharmacy (YXY2019XSGG10), Innovative Talents Training Research Project Chongqing Education Commission (CY180405), innovation and business Projects of Chongqing City (SRIEP202194) and General Program of Natural Science Foundation of Chongqing (cstc2019jcyj-msxmX0176 and cstc2017jcyjAX0029).

Appendix A. Supplementary data

Supplementary data to this article can be found online at <https://doi.org/10.1016/j.jot.2021.11.004>.

References

- [1] Molina CS, Stinner DJ, Obrensky WT. Treatment of traumatic segmental longbone defects: a critical analysis review. *JBJS Rev* 2014;2(4):01874474.
- [2] Yan B, Yin G, Huang Z, Liao X, Chen X, Yao Y, et al. Localized delivery of growth factors for angiogenesis and bone formation in tissue engineering. *Int Immunopharm* 2013;16(2):214–23.
- [3] Grgurevic L, Christensen GL, Schulz TJ, Vukicevic S. Bone morphogenetic proteins in inflammation, glucose homeostasis and adipose tissue energy metabolism. *Cytokine Growth Factor Rev* 2016;27:105–18.
- [4] Nickel J, Mueller TD. Specification of BMP signaling. *Cells* 2019;8(12):1579.
- [5] Yang YQ, Tan YY, Wong R, Wenden A, Zhang LK, Rabie ABM. The role of vascular endothelial growth factor in ossification. *Int J Oral Sci* 2012;4:64–8.
- [6] Hu K, Olsen BR. The roles of vascular endothelial growth factor in bone repair and regeneration. *Bone* 2016;6:30–8.
- [7] Beenken A, Mohammadi M. The FGF family: biology, pathophysiology and therapy. *Nat Rev Drug Discov* 2009;8(3):235–53.
- [8] Jocelynda Salvador, George E Davis. Evaluation and characterization of endothelial cell invasion and sprouting behavior. *Methods Mol Biol* 2018;1846:249–59.
- [9] Li Y, Li X, Han S, Lian W, Cheng J, Xie X, et al. Exogenous FGF-2 improves biological activity of endothelial progenitor cells exposed to high glucose conditions. *J Intervent Med* 2018;v1(1):13–8.
- [10] Siddiqui Jawed A, Partridge NC. Physiological bone remodeling: systemic regulation and growth factor involvement. *Physiology* 2016;31(3):233–45.
- [11] Uchida S, Sakai A, Kudo H, Otomo H, Watanuki M, Tanaka M, et al. Vascular endothelial growth factor is expressed along with its receptors during the healing process of bone and bone marrow after drill-hole injury in rats. *Bone* 2003;32:491–501.
- [12] Pufe T, Wildemann B, Petersen W, Mentlein R, Raschke M, Schmidmaier G. Quantitative measurement of the splice variants 120 and 164 of the angiogenic peptide vascular endothelial growth factor in the time flow of fracture healing: a study in the rat. *Cell Tissue Res* 2002;309:387–92.
- [13] Niikura T, Hak DJ, Reddi AH. Global gene profiling reveals a down regulation of BMP gene expression in experimental atrophic nonunions compared to standard healing fractures. *J Orthop Res* 2006;24:1463–71.
- [14] Groeneveld EH, Burger EH. Bone morphogenetic proteins in human bone regeneration. *Eur J Endocrinol* 2000;142:9–21.
- [15] Cho TJ, Gerstenfeld LC, Einhorn TA. Differential temporal expression of members of the transforming growth factor beta superfamily during murine fracture healing. *J Bone Miner Res* 2002;17:513–20.
- [16] Bai Y, Li PP, Yin GF, Huang Z, Liao X, Chen X, et al. BMP-2, VEGF and bFGF synergistically promote the osteogenic differentiation of rat bone marrow-derived mesenchymal stem cells. *Biotechnol Lett* 2013;35:301–8.
- [17] Diomedea Francesca, Marconi Guya Diletta, Fonticoli Luigia, Pizzicanella Jacopo, Merciaro Ilaria, Bramanti Placido, et al. Functional relationship between osteogenesis and angiogenesis in tissue regeneration. *Int J Mol Sci* 2020;21(9):3242.
- [18] Hofmann A, Ritz U, Verrier S, Eglin D, Alini M, Fuchs S, et al. The effect of human osteoblasts on proliferation and neo-vessel formation of human umbilical vein

- endothelial cells in a long-term 3D co-culture on polyurethane scaffolds. *Biomaterials* 2008;29:4217–422.
- [19] Guillotin B, Bourget C, Remy-Zolgadri M, Baille R, Fernandez P, Conrad V, et al. Human primary endothelial cells stimulate human osteoprogenitor cell differentiation. *Cell Physiol Biochem* 2004;14:325–32.
- [20] Mayer H, Bertram H, Lindenmaier W, Thomas K, Holger W, Herbert W. Vascular endothelial growth factor (VEGF-A) expression in human mesenchymal stem cells: autocrine and paracrine role on osteoblastic and endothelial differentiation. *J Cell Biochem* 2005;95:827–39.
- [21] Kanaan RA. The role of connective tissue growth factor in skeletal growth and development. *Med Sci Mon* 2006;12:277–81.
- [22] Xue Y, Xing Z, Hellem S, Arvidson K, Mustafa K. Endothelial cells influence the osteogenic potential of bone marrow stromal cells. *Biomed Eng Online* 2009;8(1):34–34.
- [23] Bouletreau PJ, Warren SM, Spector JA, Peled ZM, Gerrets RP, Greenwald JA, et al. Hypoxia and VEGF up-regulate BMP-2 mRNA and protein expression in microvascular endothelial cells: implications for fracture healing. *Plast Reconstr Surg* 2002;109:2384–97.
- [24] Tokuda H, Kozawa O, Uematsu T. Basic fibroblast growth factor stimulates vascular endothelial growth factor release in osteoblasts: divergent regulation by p42/p44 mitogen-activated protein kinase and p38 mitogen-activated protein kinase. *J Bone Miner Res* 2000;15:2371–9.
- [25] Li Peipei, Bai Yan, Yin Guangfu, Pu Ximing, Huang Zhongbing, Liao Xiaoming, et al. Synergistic and sequential effects of BMP-2, bFGF and VEGF on osteogenic differentiation of rat osteoblasts. *J Bone Miner Metabol* 2014;32(6):627–35.
- [26] Sojo K, Sawaki Y, Hattori H, Mizutani H, Ueda M. Immunohistochemical study of vascular endothelial growth factor (VEGF) and bone morphogenetic protein-2, -4 (BMP-2, -4) on lengthened rat femurs. *J Cranio-Maxillo-Fac Surg* 2005;33:238–45.
- [27] Weiss S, Zimmermann G, Pufe T, Varoga D, Henle P. The systemic angiogenic response during bone healing. *Arch Orthop Trauma Surg* 2009;129:989–97.
- [28] Bai Yan, Moeinzadeh Seyedsina, Kim Sungwoo, Park Youngbum, Yang Yunzhi Peter, Lu Elaine, et al. Development of PLGA-PEG-COOH and Gelatin-based microparticles dual delivery system and E-beam sterilization effects for controlled release of BMP-2 and IGF-1. *Part Part Syst Char* 2020;37(10):2000180.
- [29] Chaudhary LR, Hofmeister AM, Hruska KA. Differential growth factor control of bone formation through osteoprogenitor differentiation. *Bone* 2004;34(3):402–11.
- [30] Fujimura K, Bessho K, Okubo Y, Kusumoto K, Segami N, Iizuka T. The effect of fibroblast growth factor-2 on the osteoinductive activity of recombinant human bone morphogenetic protein-2 in rat muscle. *Arch Oral Biol* 2002;47(8):577–84.
- [31] Bai Y, Bai L, Zhou J, Chen H, Zhang L. Sequential delivery of VEGF, FGF-2 and PDGF from the polymeric system enhance HUVECs angiogenesis in vitro and CAM angiogenesis. *Cell Immunol* 2018;1(323):19–32.
- [32] Bronckaers A, Hilkens P, Martens W, Pascal G, Jessica R. Mesenchymal stem/stromal cells as a pharmacological and therapeutic approach to accelerate angiogenesis. *Pharmacol Ther* 2014;143:181–96.
- [33] Kankanala J, Latham AM, Johnson AP, Vanniasinkam SH, Fishwick C, Ponnambalam S. A combinatorial in silico and cellular approach to identify a new class of compounds that target VEGFR2 receptor tyrosine kinase activity and angiogenesis. *Br J Pharmacol* 2012;166:737–48.
- [34] Kempen DHR, Lu L, Heijink A, Hefferan TE, Creemers LB, Maran A, et al. Effect of local sequential VEGF and BMP-2 delivery on ectopic and orthotopic bone regeneration. *Biomaterials* 2009;30(14):2816–25.
- [35] Kanczler JM, Ginty PJ, White L, Clarke NMP, Howdle SM, Shakesheff KM, et al. The effect of the delivery of vascular endothelial growth factor and bone morphogenetic protein-2 to osteoprogenitor cell populations on bone formation. *Biomaterials* 2010;31(6):1242–50.
- [36] Zhang J, Liu Z, Li Y, You Q, Liu Y. FGF2: a key regulator augmenting tendon-to-bone healing and cartilage repair. *Regen Med* 2020;15(9):2129–42.
- [37] Hu K, Olsen BR. The roles of vascular endothelial growth factor in bone repair and regeneration. *Bone* 2016:30–8.
- [38] Charoenlarp P, Rajendran AK, Iseki S. Role of fibroblast growth factors in bone regeneration. *Inflamm Regen* 2017;37(1):10.
- [39] Maegawa N, Kawamura K, Hirose M, Yajima H, Ohgushi H. Enhancement of osteoblastic differentiation of mesenchymal stromal cells cultured by selective combination of bone morphogenetic protein-2 (BMP-2) and fibroblast growth factor-2 (FGF-2). *J Tissue Eng Regen Med* 2007;1:306–13.
- [40] Qiu Yubei, Xu Xiaodong, Guo Weizhong, Zhao Yong, Su Jiehua, Jiang Chen. Mesoporous hydroxyapatite nanoparticles mediate the release and bioactivity of BMP-2 for enhanced bone regeneration. *ACS Biomater Sci Eng* 2020;6(4):2323–35.
- [41] Brown KV, Guda, Perrien DS, Guelcher SA, Wenke JC. Improving bone formation in a rat femur segmental defect by controlling bone morphogenetic protein-2 release. *Tissue Eng A* 2011;17(13):1735–46.
- [42] Fiedler Jrg, Rderer Gtz, Günther Klaus-Peter, Brenner Rolf E. BMP-2, BMP-4, and PDGF-bb stimulate chemotactic migration of primary human mesenchymal progenitor cells. *J Cell Biochem* 2002;87(3):305–12.
- [43] Kolambkar YM, Dupont KM, Boerckel JD, Huebsch N, Mooney DJ, Huttmacher DW, et al. An alginate-based hybrid system for growth factor delivery in the functional repair of large bone defects. *Biomaterials* 2011;32(1):65–74.
- [44] Ball SG, Shuttleworth CA, Kielty CM. Vascular endothelial growth factor can signal through platelet-derived growth factor receptors. *J Cell Biol* 2007;177:489–500.
- [45] Peng H, Usas A, Olshanski A, Andrew MH, Brian G, Gregory MC, et al. VEGF improves, whereas sFlt1 inhibits, BMP2-induced bone formation and bone healing through modulation of angiogenesis. *J Bone Miner Res* 2005;20:2017–27.
- [46] Deschaseaux F, Sense L, Heymann D. Mechanisms of bone repair and regeneration. *Trends Mol Med* 2009;15:417–29.
- [47] Dudley AT, Godin RE, Robertson EJ. Interaction between FGF and BMP signalling pathways regulates development of metanephric mesenchyme. *Genes Dev* 1999;13:1601–13.
- [48] Miyazono K, Maeda S, Imamura T. BMP receptor signaling: transcriptional targets regulation of signals, and signaling cross-talk. *Cytokine Growth Factor Rev* 2005;16:251–63.
- [49] Ryo HM, Lee MH, Kim YJ. Critical molecular switches involved in BMP-2-induced osteogenic differentiation of mesenchymal cells. *Gene* 2006;366:51–7.
- [50] Diomedea Francesca, Marconi Guya Diletta, Fonticoli Luigia, Edgar C, Al-Yamani A, Apazidis A, et al. Functional relationship between osteogenesis and angiogenesis in tissue regeneration. *Int J Mol Sci* 2020;21(9):3242.
- [51] Sivaraj KK, Adams RH. Blood vessel formation and function in bone. *Development* 2016;143(15):2706–15.
- [52] Loibl M, Binder A, Herrmann M, Düttenhoefer F, Verrier S. Direct cell-cell contact between mesenchymal stem cells and endothelial progenitor cells induces a pericyte-like phenotype *in vitro*. *BioMed Res Int* 2014:395781.
- [53] Xiang Junyu, Li Jianmei, He Jian, Tang Xiangyu, Dou Ce, Cao Zhen, et al. Cerium oxide nanoparticle modified scaffold interface enhances vascularization of bone grafts by activating calcium channel of mesenchymal stem cells. *ACS Appl Mater Interfaces* 2016;8(7):4489–99.
- [54] Santoro M, Awosika TO, Snodderly KL, Hurley-Novatny AC, Fisher JP. Endothelial/Mesenchymal stem cell crosstalk within bioprinted cocultures. *Tissue Eng A* 2019;26(5–6):339–49.
- [55] Genova T, Petrillo S, Zicola E, Roato I, Munaron L. The crosstalk between osteodifferentiating stem cells and endothelial cells promotes angiogenesis and bone formation. *Front Physiol* 2019;10:1291.
- [56] Runyan CM, Gabrick KS. Biology of bone formation, fracture healing, and distraction osteogenesis. *J Craniofac Surg* 2017;8(5):1380–9.